①

DEBRIS PRODUCTION IN HYPERVELOCITY
IMPACT ASAT ENGAGEMENTS

THESIS

Stephen Karl Remillard
Captain, USAF

AFIT/GSO/ENS/90D-15

DEPARTMENT OF THE AIR FORCE

AIR UNIVERSITY

AIR FORCE INSTITUTE OF TECHNOLOGY

Wright-Patterson Air Force Base, Ohio

91 1 3 112

DTIC
SELECTE
JAN 07 1991
D
D

DEBRIS PRODUCTION IN HYPERVELOCITY
IMPACT ASAT ENGAGEMENTS

THESIS

Stephen Karl Remillard
Captain, USAF

AFIT/GSO/ENS/90D-15

THESIS APPROVAL

STUDENT: Stephen K. Remillard   CLASS: GSO 90-D

THESIS TITLE: Debris Production in Hypervelocity Impact ASAT Engagements

DEFENSE DATE: 30 NOV 90

COMMITTEE:	NAME/DEPARTMENT	SIGNATURE
Advisor/co-Advisor (circle appropriate role)	Thomas S. Kelso	*Thomas Sean Kelso*
co-Advisor/ENS Representative (circle appropriate role)	BRUCE W. MORLAN	*B.W.M.*
Reader		

i

DEBRIS PRODUCTION IN HYPERVELOCITY IMPACT

ASAT ENGAGEMENTS

THESIS

Presented to the Faculty of the School of Engineering

of the Air Force Institute of Technology

Air University

In Partial Fulfillment of the

Requirements for the Degree of

Master of Science (Space Operations)

Stephen Karl Remillard, B.A., A.A.

Captain, USAF

December, 1990

Preface

The purpose of this study is to investigate hypervelocity impact phenomenon in an attempt to find methods to minimize the production of debris fragments which result from anti-satellite engagements using kinetic energy weapons. The amount of man-made debris in space is already reaching dangerous levels, and it is conceivable that the tactical gains achieved by the use of ASAT weapons may not be great enough to offset the increased danger to spacecraft posed by the orbiting debris that will result.

I would like to thank Major Kelso for his help with the Solwind debris display. Without his help, the verification section would not have happened. I would also like to thank the Foreign Technology Division's Briefing Team for their help in providing information on RORSAT. Although they were very busy covering events in the Middle East, they took the time to get me data I otherwise might not have had. My wife, Carla, also deserves special recognition for putting up with me during the last few months.

Stephen Karl Remillard

ii

Table of Contents

List of Figures

List of Tables

AFIT/GSO/ENS/90D-15

Abstract

This study reviews laboratory experiments on hypervelocity impacts and applies the results from those experiments to predict the mass of debris produced, the number of particles, and the size distribution of the debris particles produced in an ASAT engagement using kinetic energy weapons. The three possible types of hypervelocity collisions are discussed and parameters are provided that will help predict what type of collision will occur between a given projectile and a target satellite. Once the collision type is determined, various equations are supplied which can be used to calculate debris mass, etc. Next, a notional attack between a miniature homing vehicle, similar to the one used in the successful F-15 launched ASAT, and two different satellites are examined to show the methodology for predicting the results of an ASAT engagement. Finally, suggestions are presented which can help a commander minimize the creation of debris, and thus minimize the long-term collision hazard for spacecraft resulting from ASAT engagements using kinetic energy weapons.

DEBRIS PRODUCTION IN HYPERVELOCITY IMPACT ASAT ENGAGEMENTS

I. INTRODUCTION

1.1 BACKGROUND

The increasing amount of man-made debris orbiting the earth is a growing concern for anyone wishing to operate systems in space. A collision at orbital velocities, even with a single piece of debris as small as a marble, can be catastrophic for both manned and unmanned space vehicles. This flotsam orbiting the planet is a result of years of mankind's activity in space, and is a growing threat to the safety of future space vehicles and their inhabitants.

> ...However, there is an impact danger to spacecraft which is larger than the danger due to natural meteors, and this danger is rapidly increasing. Over 30 years of spaceflight has left many dead spacecraft, empty rocket stages, and random artificial debris in orbit. Of these, the debris is far the most numerous. Explosions in orbit have left thousands of macroscopic objects in orbit as spent upper stages detonate, sometimes years after reaching orbit...Also, studies have indicated that the probability of serious damage from artificial debris is already at least an order of magnitude higher than the natural danger. The large Pageos balloon satellite was almost certainly hit and destroyed by a cataloged piece of orbital debris. Also, a space shuttle orbiter has already returned from orbit with a small crater in its windshield caused by an encounter with orbiting debris: The crater was lined with residual artificial materials. (31:261)

Due to the large impact velocities possible between orbiting debris and spacecraft (up to 15 km/sec for two objects in the same orbit traveling in opposite directions), it is impractical to shield a spacecraft against collision using any type of known armor. The large amount of energy imparted on the target during this type of impact liquifies the hardest materials. So, the only means presently available to prevent such collisions, and the resultant damage, is to prevent the creation of space debris. Even without intending to create debris, the spacefaring nations of earth have already orbited enough space junk

to present a hazard to current and future space operations. It is important to minimize the effect on the population of debris orbiting earth if space should become a battlefield and satellites are destroyed intentionally.

1.2 SPECIFIC PROBLEM

The United States Department of Defense and the Air Force are now planning for the day when hostile satellites, and possibly large numbers of Intercontinental Ballistic Missiles (ICBMs) and their reentry vehicles (RVs), will be targeted and destroyed in space. At this time, Air Force planning suggests the most likely means for conducting these attacks will be to use some type of kinetic energy weapon. (A rock is one type of kinetic energy weapon, but for the purposes of this paper, a kinetic energy weapon will be defined as any type of weapon that functions by propelling a projectile or projectiles faster than about 10,000 feet per second. The so called "Rail Gun" is an example of such a kinetic energy weapon. It uses magnetic fields, set in repulsion, to expel projectiles at great speeds.) It is probable there will be a significant volume of debris generated by a successful anti-satellite (ASAT) engagement, which could possibly disable or destroy spacecraft never intended to be harmed, such as manned space stations. When mission planning is conducted for future attacks on hostile space systems, it will be important to be capable of predicting the dispersal of such debris so that fratricide can be prevented, or at least mitigated.

It is the purpose of this investigation to determine the amount and dispostion of debris produced when a kinetic energy projectile, traveling at hypervelocity, collides with a spacecraft. From this, methods are suggested which can minimize the amount of debris resulting from an ASAT engagement. It is possible a successful attack on an enemy satellite will produce such a large amount of debris that a collision, or collisions, with friendly satellites will be unavoidable. If this is the case, a commander considering an attack gainst a hostile satellite had better know the risks before the attack begins. For example, it would be unfortunate if the residue from a Soviet Radar Ocean Reconnaissance Satellite (RORSAT) destroyed by a U.S. ASAT weapon, disabled the Hubble Space Telescope a few months after the initial attack.

2

1.3 SUB-OBJECTIVES

First, data was gathered which analyzed the impacts from hypervelocity projectiles in order to predict the interactions between the kinetic energy projectile and the target satellite. The analysis of meteor collisions and the effects of high-explosives was also helpful in predicting the outcome of engaging satellites in space. From this data, it is possible to predict the shape of the debris cloud that will result from a successful ASAT engagement. Second, a notional projectile and notional target were developed for use in illustrations and calculations. Then the size, speed, and direction of a statistically significant portion of the resultant debris was determined. In a hypervelocity collision, it is possible for hundreds of thousands of microscopic pieces of ejecta to be produced. These microscopic bits of debris weren't described or modeled in this effort because of the large amounts of time required. However, a good analysis should account for the majority of debris that is potentially dangerous so, the following calculations considered only pieces of debris which are larger than an average playground marble (1 cm. dia.).

1.4 METHODOLOGY

First, it was necessary to conduct a literature search to find available data on hypervelocity impacts, space debris, impact modeling, hydrodynamic shock effects, meteor collisions, and impact testing procedures. A search of periodical abstracts was also conducted to find any current work being done in the fields of orbital debris modeling, proposed ASAT weapons, and hypervelocity collisions. Then, an assessment was made incorporating the theoretical data obtained on hypervelocity impacts to predict the disposition the debris resulting from collisions between selected satellites and kinetic energy weapons. The target satellites chosen were: one that will likely be a target early in any major conflict, a RORSAT; and one that was successfully destroyed by kinetic energy weapon, the Solar Observation satellite (Solwind).

The result of this research is a methodology for predicting the total mass, number of debris particles, and the distribution of mass among the debris particles resulting from the collision of a kinetic energy projectile with a spacecraft.

II. Literature Review

2.1 INTRODUCTION

To determine the disposition of debris from an ASAT engagement, it must first be determined what happens during the actual collision between the attacking projectile and the target satellite. Will the target be totally destroyed or will the projectile leave a crater of some size in an otherwise intact satellite? Will the fragments of debris that result be of uniform size, shape, or traveling with similar velocities? Can the fragments' direction of travel be predicted? These are the questions that must first be answered before any suggestions can be made as to how debris production can be minimized. The following paragraphs review literature on hypervelocity impact phenomenon. This data will provide the theoretical basis on which to develop a methodology to predict debris production. Specifically, the discussion covers the following topics:

2.1.1 Target-Projectile Interaction. When a kinetic energy weapon collides with a satellite, what happens? Is the satellite always destroyed? Is the projectile always destroyed? Is it possible that the projectile could bounce off of the target rather than penetrate it? Under what circumstances will a projectile merely pass through a target, leaving a hole the size of the projectile?

2.1.2 Debris Disposition. What will be the disposition of debris that results from an ASAT engagement? That is, how much debris mass will be generated, how many debris fragments will be created, and what will be the fragments' new direction of travel? Is there an advantage in using a large or small projectile to minimize debris creation?

2.1.3 Definitions. Throughout the following discussion, some key terms will be used repeatedly. This will be a good time to specify their intended meaning for this effort.

PROJECTILE: The fast moving object which has been intentionally launched against the target satellite with the purpose of destroying it. Also referred to as M_1 (Mass 1).

TARGET SATELLITE: The single satellite that the projectile is intended to collide with and destroy. Also referred to as M_2 (Mass 2).

FRIENDLY SPACECRAFT: Man-made space systems, currently orbiting the earth. which may inadvertently be struck by the projectile or by the debris that results from the ASAT engagement. These spacecraft were never intended to be damaged in any way.

CATASTROPHIC COLLISION: Both the projectile and the target satellite are totally destroyed and converted to debris fragments. This happens when the projectile and the target satellite have roughly the same mass.

NONCATASTROPHIC COLLISION: The projectile damages the target satellite and produces some debris. The projectile may be destroyed, but the target satellite is left largely intact. This type of collision occurs when the projectile is very much smaller than the target satellite.

2.2 DISCUSSION

2.2.1 Target-Projectile Interaction. The literature suggests that when a projectile, traveling at orbital velocities, collides with another object, the projectile will:

1. Pass through the target, leaving a hole in the target and the projectile partially intact (Noncatastrophic collision).

2. Penetrate the target to some depth and cause a crater to be formed (Noncatastrophic collision).

3. Utterly destroy the target (Catastrophic collision).

Apparently, the kinetic energy of projectiles traveling at hypervelocity is just too great to allow for any ricochets. Objects in orbit around the earth are necessarily moving very fast (minimum of about 7 km/sec to maintain a circular orbit); otherwise they won't remain in orbit. It is because of this fact that collisions between objects in orbit are assumed to be "hypervelocity" impacts (hypervelocity being greater than 3 km/sec).

"The average impact velocity of 10 km/sec ensures that almost all of the earth-orbiting objects will exhibit hypervelocity impact characteristics when they collide...A crater, or hole, will be formed, the molten ejected mass coalescing into more or less spherical particles." (15:2639)

Cintala describes a typical hypervelocity impact:

> In the very earliest stages of the event, as the projectile makes contact with the target, two shock waves are formed; one travels into the target, while the other moves back into the projectile. The combination of high shock pressures (typically on the order of hundreds of kilobars to megabars for the events considered important here) and free surfaces yields violent decompression and high-velocity ejection of molten and vaporized material, giving rise to a hydrodynamic process generally referred to as "jetting" (Gault et al. 1968)...By the time the shock wave reaches the trailing end of the projectile, the majority of the transferral of energy to the target is complete. The time elapsed from initial contact to this stage in the event is on the order of the time taken for the shock wave to traverse the length of the projectile. For a basalt meteoroid of one meter in diameter impacting a basaltic target at 5 km/sec, this will occur within 10^{-4} sec. (5:580)

So, for the given 1-meter diameter projectile traveling at 5 km/sec, it will pass through any object which is thinner than about 0.5 meters (10^{-4} sec $\times$ 5 km/sec = .0005 km). This is assuming the "back" end of the projectile doesn't slow down appreciably until the shock wave passes through it.

In his analysis of debris created from hypervelocity impacts, Kessler described collisions as either catastrophic or noncatastrophic and doesn't try and specify the type of damage done to the target during a collision.

Hypervelocity impacts into solid structures can be divided into two groups: catastrophic and noncatastrophic. A non-catastrophic collision results from the collision of two masses M_1 and M_2, where M_1 is much smaller than M_2 by an amount

$$M_2 > T' \times M_1 \qquad\qquad (1)$$

where T' is a function of the impact velocity and the structure and materials of M_1 and M_2. (15:2640)

For the purposes of this paper:

M_1 = Mass of projectile

M_2 = Mass of Target

T' = Constant derived from materials in M_1 and M_2

For ASAT missions of the near future, it seems likely that a relatively small, but very fast moving projectile, will be the weapon of choice used against the much larger target satellites. The only U.S. ASAT weapon ever successfully tested was a kinetic energy weapon of this type (see Appendix A). The Soviets also developed and extensively tested an ASAT weapon which used shrapnel from an explosion to disable the target satellite. In addition to the ASAT weapons already developed, the technology now being developed to counter a ballistic missile attack is directly applicable to attacking satellites. These so-called "Brilliant Pebbles" (small, guided kinetic energy weapons) are the type of weapon thought most likely to offer a real chance to defeat enemy missiles and warheads. Since this is the most promising technology to defeat ICBMs, it is likely that something similar to "Brilliant Pebbles" will be used to destroy enemy satellites. This "small and fast" type of ASAT projectile is discussed by Roark in his research on "Active Pellets" (23:9). Roark researched ASAT projectiles that weigh about 10 grams and contain chemicals that corrode the target on impact. It is thought that these active chemicals will make the small projectile as effective in destroying the target satellite as more massive projectiles.

The emerging rail-gun technology also has direct application to ASAT engagements. In an article appearing in *Aviation Week & Space Technology*, "Researchers at Sandia National Laboratories are testing an electromagnetic coil gun that they say could be developed

into an economical means for launching small payloads into orbit" (12:88), a device is discussed which could possibly be used as an ASAT weapon. The first full-scale launcher is expected to be capable of putting a 61-kg payload into low-earth orbit. It is feasible these payloads could be directed against satellites in orbit, which would mean this ground-based payload launcher could possibly be used as a ground-based ASAT weapon.

When assessing the disposition of debris from an ASAT engagement, it is important to know what type of collision will occur between the projectile and the target. Based on the type of ASAT weapons already developed and the research currently being done, it appears likely that the type of weapon to be used against satellites will be some small, fast-moving kinetic energy projectile.

2.2.2 Debris Disposition.

In almost every article that was found on the disposition of debris in space, one author was cited as a source, almost without exception. Donald J. Kessler has written several articles in this area, and is apparently highly regarded. Articles that he has written include: "Collision Avoidance in Space," "Collision Frequency of Artificial Satellites: The Creation of a Debris Belt," "Derivation of the Collision Probability Between Orbiting Objects: The Lifetimes of Jupiter's Outer Moons," "Ground Radar Detection of Meteoroids in Space," and "Junk in Space." These articles, in general, are concerned with how debris in space will affect space operations, and not ASAT engagements in particular, but there is much in common between the two areas of interest.

2.2.2.1 Debris Mass From A Noncatastrophic Collision.

There is general agreement in the literature that the total mass of material which is ejected from a hypervelocity collision is a function of collision speed and the density of the target and projectile. There also seems to be a underlying assumption, in many of the studies, that basalt and spacecraft materials react similarly during hypervelocity impacts.

Moore (19:43) uses a fairly complex formula to calculate the mass of debris ejected from blocks of basalt hit by metal projectiles. But to use it, the densities of the projectile and target must be known as well as the target's kinetic energy. For laboratory experiments it probably works well. Unfortunately, the density of a complex structure like a satellite

8

may be difficult to calculate accurately and a good value for the projectile's kinetic energy at the time of impact with the target in orbit may be difficult to predict precisely. The experimental results show that the mass ejected (M_e) from craters produced by hypervelocity and high-velocity projectile impact with basalt increases with the projectile energy (E_p), and the square root of the ratio of projectile and target densities $(R_p/R_t)^{1/2}$ (19:43).

$$M_e = 10^{-10.613}[(\rho_p/\rho_t)^{1/2}E_p]^{1.189} \tag{2}$$

where:

M_e = Ejected mass

E_p = Projectile energy

ρ_p = Projectile density

ρ_t = Target density

By assuming that all objects of interest will collide at about 10 km/sec, and that all objects in space have similar densities and deformation characteristics, Kessler calculates the debris mass created by a noncatastrophic in the following way:

In noncatastrophic collisions, only M_1 is destroyed, and a crater is produced in M_2, ejecting a total mass of M_e, which can be expressed as

$$M_e = T \times M_1 \tag{3}$$

where T is also a function of the impact velocity and the structure and materials of M_1 and M_2. (15:2640)

Kessler (15:2640) then goes on to provide a table of values for T and T' for some common spacecraft materials. T is the ratio of ejected mass to projectile mass in a noncatastrophic collision at 10 km/s. T' is the minimum ratio of target mass to projectile mass causing catastropic disruption at 10 km/s.

Table 1. Hypervelocity Impact Parameters

Material	T'	T
Basalt	25,000	500
Glass	120,000	2,000
1100-0 aluminum	2,600	130
Spacecraft structure	$> 115^1$	115

For the materials that generally make up spacecraft, $T = 115$ and $T' > 115$. This suggests that at 10 km/sec, if the spacecraft is at least 115 times more massive than the projectile, a noncatastrophic collision occurs. If the spacecraft is less than 115 times the mass of the projectile, a catastrophic collision occurs. Thus, for collisions between earth-orbiting objects, the following relationship was adopted(15:2640):

$$M_e = 115 \times M_1 \qquad (4)$$

This formula provides an estimation for debris mass knowing only the mass of the projectile.

2.2.2.2 Debris Mass from a Catastrophic Collision.
Using the same simplifying assumptions made for calculating debris mass from a noncatastrophic collision, Kessler calculates the mass of debris (M_e = mass of ejected material) resulting from a catastrophic collision in the following way:

> If M_1 is larger than the amount given in Equation 1, then not only is a crater produced in M_2, but the entire structure of M_2 begins to fragment. This process is referred to as a catastrophic collision. These additional fragments are usually larger than the fragments from the crater and are ejected at a much slower velocity. The mass ejected from a catastrophic collision is
>
> $$M_e = M_1 + M_2 \qquad (5)$$
>
> The ejected mass has also been shown to be proportional to the impact kinetic energy [Moore et al., 1965; Dohnayi, 1971]. Thus the values for T and T' will vary as V_2. (15:2640)

---

[1] No tests have been performed to obtain this value. This lower limit follows from the definitions of T' and T.

When considering the creation of orbital debris as a bad thing, this would then be the worst case for any ASAT engagement. All of the target and all of the projectile are converted to debris.

2.2.2.3 Number and Shape of Debris Particles Created. "The number of small fragments of mass M and larger ejected from a noncatastrophic collision can be expressed as:

$$N = K(M/M_e)^{\eta} \tag{6}$$

where K and η are constants" (15:2640). For this equation, N is the number of ejected fragments with mass M and larger, K is a constant determined by the type of materials in the colliding objects with the units of grams$^{1/2}$/cm$^{7/6}$ (for spacecraft, $K \simeq 0.8$), η is also a constant determined by the materials in the colliding objects (for spacecraft, $\eta \simeq -0.8$), and M_e is the mass ejected during the collsion.

Kessler then makes some comparisons between debris from spacecraft collisions and asteroid collisions and asserts, "When normalized by the total ejected mass, as in Equation 6, the distribution of fragments from spacecraft structures looks very similar to that of basalt." Then using the values for K and η obtained from tests on basalt (the primary material found in asteroids), Kessler derives an equation for the number of fragments resulting from a collision between earth-orbiting objects (15:2640). The number of fragments of mass M and larger resulting from the collision is given by

$$N = 0.8(M/M_e)^{-0.8}. \tag{7}$$

2.2.2.4 Size and Velocity of Ejected Particles. Cintala, M. J. *et al.* suggest that the ejecta that comes from material nearest the center of an impact crater will be the smallest of all the debris that results from the collision and it will be moving at the highest speed.

In general, the highest velocity ejecta from an event in a homogeneous target originate near the point of impact (the jetted phases and very earliest ejecta following the demise of the projectile), while that with the lowest veloctiy come from near the rim region (e.g., Stöffler *et al.* 1975: Oberbeck 1975: Oberbeck and Morrison 1976). (5:582)

In a coherent target, higher peak shock stresses imply smaller particle sizes due to fracturing (Gault *et al.* 1963, Öpik 1971; Oberbeck 1975). In general, since ejection angles appear to be relatively constant during the excavation stage of a cratering event (Oberbeck and Morrison 1976; Ivanov 1976), the smallest fragment should be ejected at the highest velocities and travel the greatest distances; the larger fragments, having experienced lower peak pressures, will travel shorter distances from the crater (Oberbeck 1975; Cintala *et al.*). Thus, the coarsest fragment should be found near the crater rim, with the average size decreasing as a function of increasing radial distance. (5:583)

Although there is agreement that the fastest debris particles are generated from the point nearest the center of the collision, there is some disagreement as to the absolute velocity of the ejected particles. From Cintala (5:581): "The jetted mass is rapidly accelerated to velocities well in excess of the impact velocity, and is composed of material contributed from both the target and the projectile." As you move outward toward the rim of the crater, the material will be ejected more slowly, and in larger chunks.

Kessler differs from Cintala in his estimation of the speed of the ejected material. When discussing hypervelocity tests conducted by Langley Research Center, he states "The velocities of fragments, measured from a 400 frame/sec film, were found to be very slow, about 10-30 m/s. Most of the fragment mass from basalt targets is slower than 100 m/s" (15:2640). This is considerably less than "...velocities well in excess of the impact velocity" (10 km/sec) predicted by Cintala.

2.2.3 Velocity of Debris Particles. Henderson B. J. (11:29) provides a equation that relates the projectile's original velocity to the velocity components of the ejected fragments. His equation generates a debris "spray cone" with the greatest number of fragments being deflected at the angle specified in the velocity ratio of V_x/V_y:
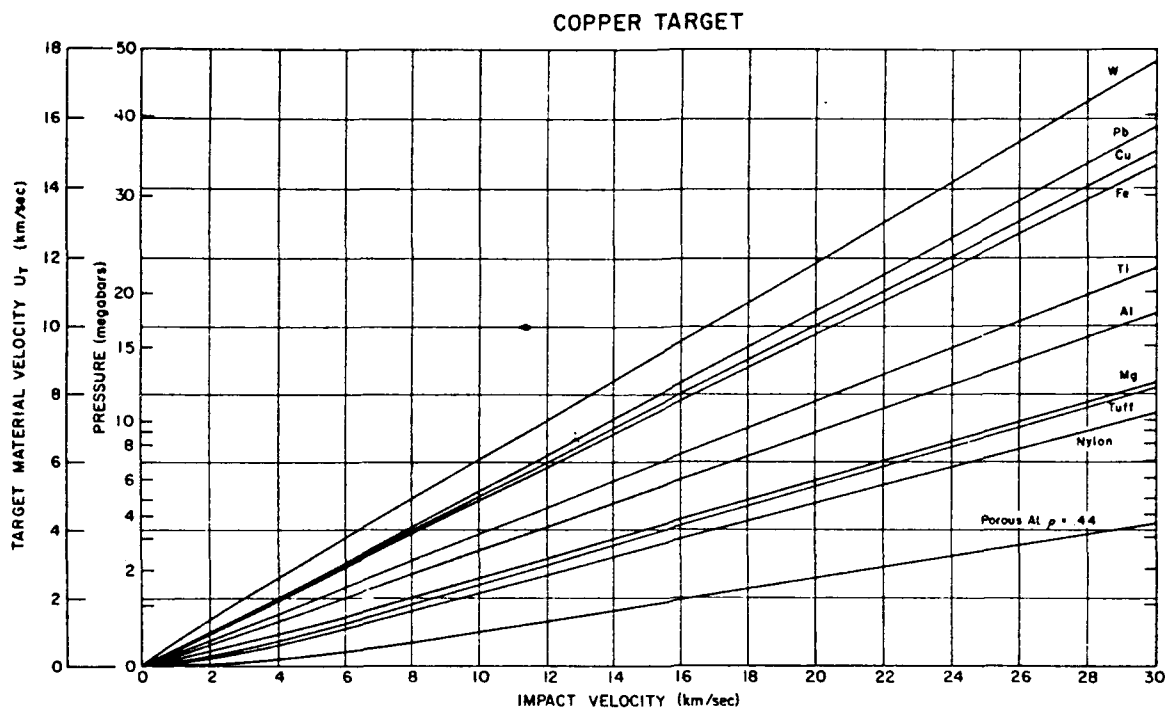
Figure 1. Velocity Comparisons
(20:14)

$$V_x/V_y = d(0.01 \times V_o + 0.127) \tag{8}$$

where:

V_x = Velocity (km/s) Perpendicular to V_o

V_y = Velocity (km/s) Parallel to V_o

V_o = Initial Velocity Vector of Projectile

d = Projectile Diameter (cm)

13

2.3 SUMMARY

When a projectile collides with a satellite at orbital velocities, the outcome of the collision is determined largely by the relative masses of the projectile and target. If the projectile and target are roughly the same size (within a factor of 100) a catastrophic collision will result. This means that all of the target and all of the projectile are converted to debris. Otherwise, some amount of debris will be generated as a function of the mass and velocity of the projectile. A more massive, or faster moving, projectile will generate more debris, all other factors being equal.

The literature review also provided several mathematical formulations which predict the disposition of debris which results from an ASAT engagement. The accuracy of the formulations, as with most, is dependent on the detail of information available about a particular collision.

III. Hardware

This chapter describes the actual spacecraft and kinetic energy weapon projectiles that currently exist and are the most likely to be involved in an ASAT engagement. Each is described in general terms in this chapter to give the reader a general idea of the size and type of objects involved. However, for the curious, detailed information can be found in Appendices A and B.

After describing the actual hardware in use, some simplifying assumptions are made about the size and composition of the projectile and target to be used for calculations within this model. For example, both objects are homogeneous solids with ideal physical characteristics. That is, there are no cracks or other imperfections that will change the way they react during hypervelocity collisions. Then, the notional hardware used for this effort are presented.

3.1 THE PROJECTILE

To attack a satellite in orbit with a kinetic energy weapon, some type of projectile is required. The projectile may be launched by an electromagnetic rail gun, on the front of a missile, or possibly by some other type of propulsion not yet developed, but after it is launched the projectile carries with it all of the energy that can be directed against the target. The projectile must be large enough to impart sufficient energy upon the target to achieve the desired level of damage, yet small enough to be launched. And of course, it must hit the target. Close counts for nothing when using kinetic energy weapons. The energy stored in the projectile that actually causes damage t he target is kinetic energy (KE) and can be calculated using the fundemental relationship:

$$KE = 1/2MV^2 \qquad (9)$$

where:

M = mass of the projectile

V = velocity of the projectile

The impact energy of a piece of debris in low-earth orbit equals:		
Size	**Type (example)**	**Corresponding object**
1mm	small fragment	= bottle of beer (1 kg) at 100 km/h
1cm	bolt	= car (800 kg) at 100 km/h
10cm	spent hatch	= train (500 tons) at 100 km/h
1 m	old satellite	= aircraft carrier (90,000 tons) at 100 km/h

Table 2. Impact Energy Comparison
(30:130)

For example, if a projectile's mass is about 10 kilograms (it will weigh about 22 lbs on earth) and is traveling at orbital velocity (about 7 km/sec) it will possess about 245 million joules of energy. For comparison, a two-ton automobile traveling at 100 mph has about 181 million joules of kinetic energy (see Table 2 for more energy comparisons).

As with the energy calculation above, the mass and velocity of the projectile determines what will happen during a hypervelocity collision. A large projectile used against a target of roughly the same mass will result in a catastrophic collison where both the target and projectile are totally destroyed. A small projectile impacting a very much larger target may result in little or no damage to the target satellite. So, when considering what size of projectile to use for calcualtions within this computer model, it is necessary to cl oose a projectile which is closely approximates the type of projectile that will actual be used in an ASAT engagement. To that end, the projectile used for making calulations in this effort is very similar to the miniature homing vehicle used in the only U.S. kinetic energy ASAT weapon ever successfully tested.

← Direction of Travel

Single Shot, Solid
Rocket Motors

30.5 cm

← 33 cm →
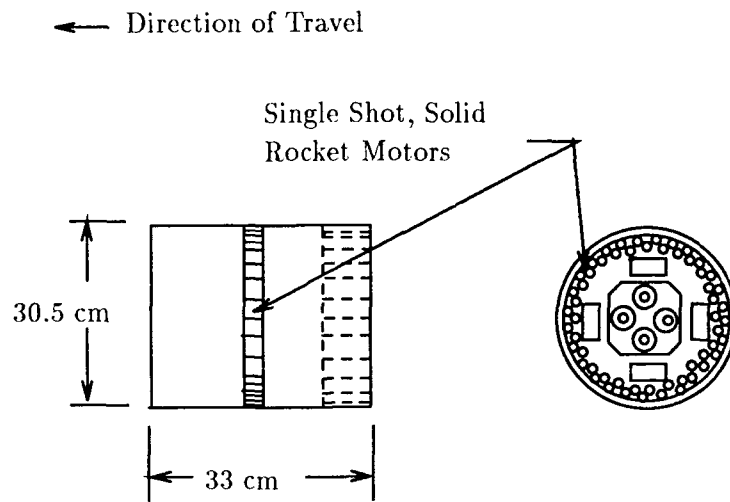
Figure 2. F-15 Launched Miniature Homing Vehicle

In September 1985, the U.S. Air Force fired a miniature homing vehicle into orbit onboard a modified short-range attack missile (SRAM) launched from an F-15 fighter jet. The miniature homing vehicle succeeded in tracking and intercepting a scientific satellite that had outlived its useful lifetime. The projectile had a mass of 15.88 kg (35 lbs) and contained a laser gyro for guidance and eight cryogenically cooled infrared detectors for homing. Midcourse corrections were provided by single-shot solid motors that fire out the vehicle's side (see Figure 2). The projectile was about 33 cm (13 inches) long, 30.5 cm (12 inches) in diameter, and weighed about 35 pounds (for details about the F-15 based ASAT program, see Appendix A).

Direction of Travel

30.5 cm 25.4 cm

33 cm
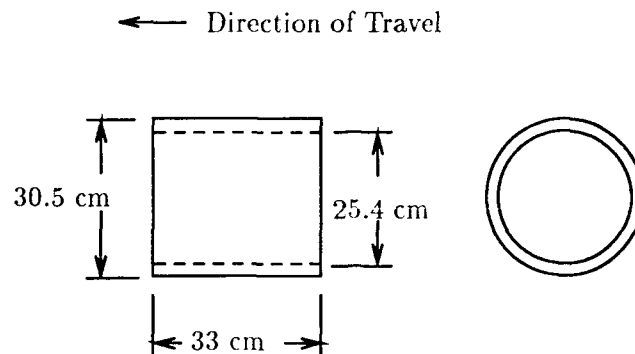
1) Mass = 16 kg (35 lbs)

2) Made of aluminum (Density = 2.71 g/cubic cm)

3) Volume = 24,125 cubic cm

Figure 3. First Simplification

For the purposes of this study, it is unimportant how the projectile is guided, or how it got into space. So, details of the projectile's construction can be disregarded to simplify the computer model which will be developed. These simplifications will make it possible to use formulae developed in labaratories, using homogeneous projectiles against homogeneous targets, to predict the outcome of the notional ASAT engagement. The operational projectile weighed 35 pounds, which works out to be 15.88 kilograms. However, 15.88 is a cumbersome number and since metric units will be used in this effort, the notional projectile will be mass an even 16 kilograms.

The first simplification developed was to model the projectile as a hollow right-circular cylinder made of homogeneous aluminum with the same shape and dimensions, and about the same mass, as the miniature homing vehicle used in the successful F-15 ASAT test. Essentially, the first simplification was an aluminum sleeve about the size of a large coffee can. Unfortunately, many of the equations used for predicting target penetration and the size of holes formed in thin plate targets uses the radius of the projectile to make the predictions. These formulae presume the projectile is a homogeneous solid, and make no allowances for hollow projectiles, so the first simplification of the projectile was discarded.

←——— Direction of Travel

30.5 cm

|← 33 cm →|
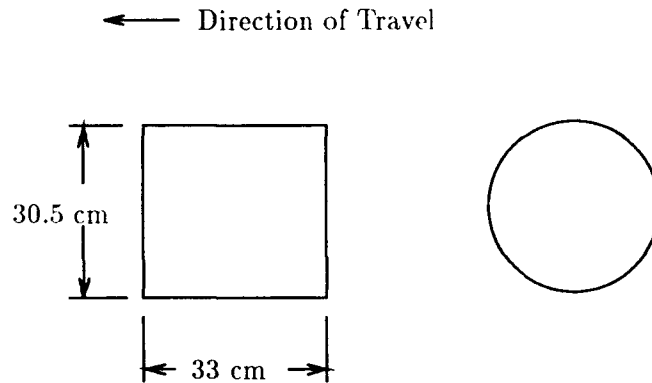
1) Mass = 16 kg (35 lbs)

2) Density = 0.66 g/cubic cm

3) Volume = 24,125 cubic cm

Figure 4. Second Simplification

The second simplification developed used the same outer dimensions of the Miniature Homing Vehicle, but assumed it was a homogeneous solid whose density would yield the proper mass for the volume of the projectile. For a right-circular cylinder with a diameter of 30.5 cm and a height of 33 cm, it will have a volume of 24,125 cubic centimeters (Vol $= \pi R^2 H$). To achieve the desired projectile mass of 16 kg, the density of the notional projectile material would be 0.66 grams/cu cm. This density is about the same density of a hardwood such as oak. This simplification worked out fairly well until the results from different methods of calculating debris mass were compared and no clear results could be predicted. The problem was found to be in the value of the constants used for the materials in the hypervelocity experiments. Most of the experiments used projectiles made of some type of metal. Aluminum projectiles were very common. The density of aluminum is 2.7 grams/cu cm. This density is significantly different than the density of 0.66 grams used for the second projectile simplification. This density difference led to wildly varying results from formula to formula. Since it would be necessary to conduct hypervelocity impact experiments using wooden projectiles to obtain the necessary values for the needed constants, the second projectile simplification was also discarded.

19

← Direction of Travel

19.6 cm

19.6 cm
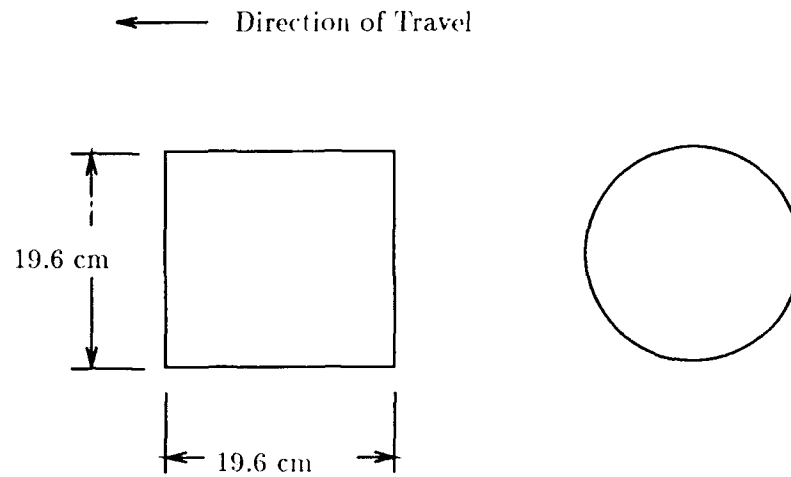
1) Mass = 16 kg (35 lbs)

2) Density = 2.71 g/cubic cm

3) Volume = 5,900 cubic cm

Figure 5. Notional ASAT Projectile

Finally, to use the forumulae that are available, the notional projectile is defined to be a solid, homogeneous right-circular cylinder made of aluminum. Since the miniature homing vehicle is less dense than solid aluminum, to keep the projectile mass as 16 kg, the notional projectile must be smaller than the actual miniature homing vehicle. Thus, the notional projectile is only 19.6 cm in diameter, and is only 19.6 cm long. But, it is now a homogeneous solid and is composed of a material commonly used in hypervelocity experiments. This final simplification will allow the use of most of the available formulae and thus give the best results.
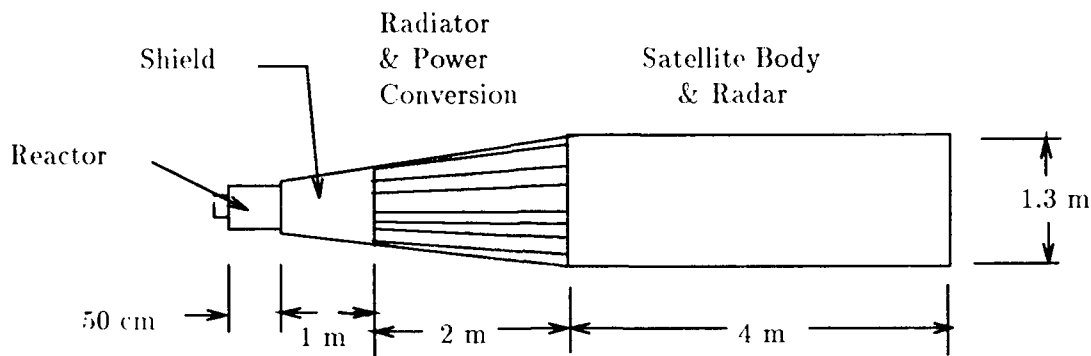
Figure 6. Soviet Radar Ocean Reconnaissance Satellite
(3:5)

3.2 THE TARGET

In the event the United States becomes involved in a war with another space power, one of the first actions that will probably be undertaken is an attempt to neutralize the reconnaissance satellites controlled by the hostile nation. Without the intelligence data provided by these eyes in the sky, a nation's ability to wage war will be significantly hampered. Force disposition, orders of battle, weather over the target, and other intelligence data required to properly conduct military operations will no longer be readily available. Mission planning will have to rely on older and slower types of intelligence gathering such as scouts, spies, and reconnaissance aircraft (if they are still available).

At this time, the Soviet Union is the only hostile space power that the United States could conceivably go to war with in the near future. Therefore, it is probably a Soviet reconnaissance satellite that the U.S. ASAT effort will first be directed against. Of primary importance among Soviet orbiting recconnaissance assets are the ELINT ocean surveillance satellites.

The objectives of the Soviet ocean reconnaissance network are to detect, identify, and track U.S. and Allied naval forces and to relay this information in real time directly to Soviet naval and air elements. In peacetime and periods of world tension, this information enables Soviet military leaders to monitor the movements of Western naval forces and to warn of unusual or threatening formations. Both Warsaw Pact and NATO naval exercises are routinely monitored by these Soviet satellites (8:53). In wartime, ocean reconnaissance data will help direct Soviet weapons platforms or the munitions themselves against enemy vessels (33:1).

The Soviet ocean surveillance program is comprised of two complementary satellite systems: the Radar Ocean Reconnaissance Satellites (RORSATs) and the ELINT Ocean Reconnaissance Satellites (EORSATs). Both systems are orbited by the SL-11 launch vehicle from Tyuratam and are inserted into orbital inclinations of 65 deg to permit virtually complete surveillance of all strategic waterways. Historically, the EORSATs have flown at altitudes between 400 and 445 km while RORSATs have maintained a mean altitude of only 255 km in a comporomise of radar power, probability of detection, and atmospheric drag. Both RORSATs and EORSATs often work in coplanar pairs, but the intitial spacing between the plane of the RORSATs and the plane of the EORSATs is approximately 145 deg, although this spacing gradually increases with time due to orbital perturbation effects. (13:113-117)

In 1978, a JCS Directive was issued with a prioritized list of space targets to be destroyed in the event of war. Within this list, the ocean reconnaissance satellites were given top priority and "should be destroyed as soon as possible." All other space targets on the list were to be destroyed within 48 hours (28:208). It is because of the importance of this type of satellite that a RORSAT will be used as the target model for the notional ASAT attack in this effort.
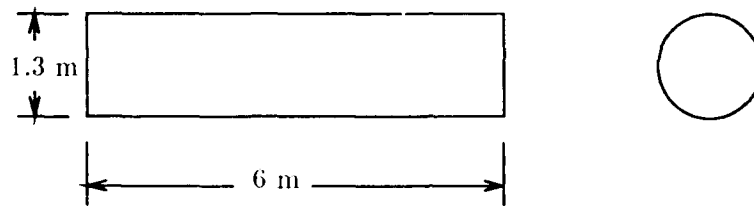
1) Mass = 4,000 kg

2) Density = 500 kg/cubic meter

3) Volume = 7.96 cubic meters

Figure 7. First Simplification

As with the projectile, to make this computer simulation more manageable, the shape of the target was also simplified somewhat. The first simplification is to make the notional target a simple right-circular cylinder with about the same dimensions of the RORSAT. The problem with this configurations is that if the notional target is to have a mass of 4,000 kg, its density will be only 500 kilograms per cubic meter, which is about the density of wood. To make the density of the target consistent with materials found in potential ASAT targets, the notional target will be smaller than the RORSAT in order to make its density roughly that of aluminum.
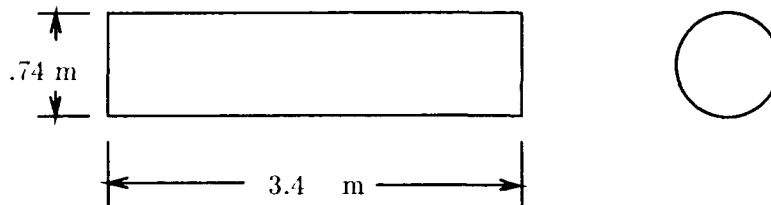
1) Mass = 4,000 kg

2) Density = 2,710 kg/cubic meter

3) Volume = 1.48 cubic meters

Figure 8. Notional Target

This further modified version of the target will be referred to as the notional target and is a simple right-circular cylinder which is 3.4 meters long and has a diameter of 0.74 meters. Its mass will be the same as the operational RORSAT at 4,000 kg.

IV. The Collision

This chapter will describe what happens during a hypervelocity impact and try to give the reader an understanding of the three major types of hypervelocity collisions. For the following calculations, the target is assumed to be in a circular orbit with an altitude of about 250 km, and the projectile will impact the target at 10 km/s. The following three cases should cover all of the types of collisions that might occur between an ASAT projectile and its target. The three types of collisions are:

Thin Plate: A thin plate collision occurs when the target is too thin to stop the projectile. There is a maximum thickness which will allow the projectile to penetrate the target. This thickness will vary with the shape, mass, and velocity of the projectile and, to a lesser degree, the material of the target. This type of collision can be thought of as a rock falling through a sheet of aluminimum foil. Or, in the case of spacecraft, this collision is likely to occur when a small projectile hits a solar panel.

Thick Target (also called semi-infinite): A thick target collision can be best visualized as a meteroid striking a planet. The projectile is very small, when compared to the target. For spacecraft, this type of collision is likely to occur when a small projectile hits the body of a large satellite.

Small Target: A small target collision can be visualized by two planets of equal size colliding. The absolute size of the target does *not* determine whether a small target collision will occur. It is the target's size *relative to the projectile* that is important. When this type of collision occurs, the target and the projectile are destroyed.

4.1 COLLISION CRITERIA

Before it can be specified what type of collision will occur between any given projectile target combination, two major factors must be determined. First, how far will the projectile penetrate into the target? And, secondly, what is the ratio of projectile's mass to the target's mass? These two factors will determine which of the three types of collisions will occur.

4.1.1 Penetration Depth. During a hypervelocity collision, the projectile will continue to penetrate the target until the shock wave generated by the initial impact traverses the length of the projectile. The longer the projectile, the deeper the hole. And, the faster the projectile is moving the farther it will penetrate the target before the shock wave in the projectile has reached the trailing end. This brings up the question; how fast does the shock wave travel in the projectile? According to Chou (6:63) and Miller (18:230), for homogeneous materials the velocity of the shock wave (also referred to as the sonic velocity or C) is found by dividing Young's modulus (E) for the projectile's material by the density (ρ_p) of the projectile's material

$$C = \sqrt{E/\rho_p} \tag{10}$$

For aluminum (which is what the notional projectile is made from)

$E = 70$ G Pascals

$\rho_p = 2,710$ kg/cu. meter

Thus, for the notional projectile (see Figure 5)

$$C = \sqrt{7.0 \times 10^{10}/2,710} = 5,080\,\text{m/sec} \tag{11}$$

the shock wave will travel at 5,080 meters per second through the projectile.

Since the projectile is 19.6 cm long, it will take $.196/5,080 = 3.86 \times 10^{-5}$ seconds for the shock wave to travel the length of the projectile (L_p). When traveling at 10 km/s. the projectile will cover a distance of $10,000 \times 3.86 \times 10^{-5} = 0.39$ meters in that time.

So, a first cut approximation for penetration depth (P_t) would be

$$P_t = V_p(Lp/C) = 0.39 \, \text{m}. \tag{12}$$

However, the front of the projectile is being eroded so the interface between the projectile and the target is moving into the target at only about one-half of the projectile's original velocity. But, on the other hand, the shock wave created in the target by the collision travels faster than the interface between the projectile and target materials so the final crater depth will be greater than the distance covered by the interface. The final crater wall occurs where the pressure in the shock wave is equal to the target material's yield stress (16:194).

In their work with hypervelocity impacts into beryllium, graphite, and lucite targets, Diedrich and Loeffler (7:44) take these problems into account and produce the following equation for the penetration depth normalized by the projectile diameter:

$$P_t/D_p = \gamma \, (\rho_p/\rho_t)^{1/2} \, (V_p/C)^{2/3} \tag{13}$$

where:

P_t = Penetration Depth

D_p = Diameter of Projectile (19.6 cm for the notional projectile)

γ = Constant Dependent on Type of Materials ($\gamma = 2$ for a wide range of materials)

ρ_p = Density of Projectile (2,710 kg/cu. m)

ρ_t = Density of Target (2,710 kg/cu. m)

V_p = Velocity of the Projectile (10 km/s or 10,000 m/s)

C = Sonic Velocity of Target Material (5,080 m/s for aluminum)

Substituting in the above values gives

$$P_t/D_p = 2 \, (2,710/2,710)^{1/2} \, (10,000/5,080)^{2/3} = 3.14 \tag{14}$$

27

Thus, the ratio of penetration depth to the projectile's diameter is 3.14, or for the notional projectile

$$P_t = D_p \times 3.14 = 61.5\,\text{cm}. \tag{15}$$

Another approximation for penetration depth is provided by Swift (35:217) where he states that penetration depth (P_t), in a semi-infinite target, goes as the 2/3 power of the projectile velocity (V_p). Both of these penetration equations apply only to "chunky" projectiles with their dimensions of height, width, and depth all about the same. A sphere is the perfect chunky projectile. These equation are appropriate for this effort because the notional projectile qualifies as a chunky projectile (length = 19.6 cm, diameter = 19.6 cm):

$$P_t/D_p = (\rho_p\,K/4)^{1/3}\,V_p^{2/3} \tag{16}$$

where:

P_t = Penetration Depth

D_p = Diameter of Projectile (19.6 cm for the notional projectile)

ρ_p = Density of Projectile (2.71 g/cc)

K = Constant (0.5 $\times$ 10^{-10} cc/erg)

V_p = Velocity of the Projectile (10 km/s or 10^6 cm/s)

Substituting in the above values gives

$$P_t/D_p = (2.71\,(.5 \times 10^{-10})/4)^{1/3}\,(10^6)^{2/3} = 3.24 \tag{17}$$

or

$$P_t = D_p \times 3.24 = 63.5\,\text{cm}. \tag{18}$$

Diedrich's equation predicts that the notional projectile will be able to penetrate a thick (semi-infinite) target to a depth of 61.5 cm. On the other hand, Swift's equation predicts the penetration to be just slightly more at 63.5 cm. This is very good agreement considering the equations use different parameters to make the calculation. For the purposes of future calculations, the value of 62.0 cm will be choosen as penetration depth (P_t).

So, our projectile can penetrate a thick target to a depth of 62 cm. But this is not the whole story. A projectile will actually penetrate deeper into a thin plate target than a thick target, if they are both made from the same materials. This is because the shock wave, reflecting off the back surface of the thin plate target as a rarefaction wave, gets involved in the collision and adds to the pressure generated by the initial shock wave. In a thick target, the travel time for the reflected wave is too great to be involved in creating debris. According to Fish and Summers (9:17), "It has been customary to predict that a thin target will be perforated by a projectile if its thickness is 1.5 times the penetration which the projectile would make in a semi-infinite slab of the same material." So, for a target to be penetrated by the notional projectile, and thus qualify as a thin plate target, it must be less than 0.93 m (62 × 1.5 = 93.0 cm) thick.

These figures can only be used as a close approximation because predicting penetration depth cannot be done precisely.

> The precise target-impact conditions required to just perforate the target have a small but definite statistical component. For this reason, no specific set of target-impact conditions can be specified as the limit for target perforation. (35:222)

Also, if the projectile is not a chunky projectile, it may be a long thin rod for example, the foregoing equations do not apply. Hypervelocity impacts with long rod projectiles are significantly different than impacts with chunky projectiles and will not be considered in this effort.

4.1.2 Target-Projectile Mass Ratio. When deciding what type of collision is likely to occur, the other factor that must be considered is the ratio of the projectile's mass to the target's mass. If the mass of the projectile is approximately the same as the mass of the target (within a factor of 115 (15:2640)), the target will not have sufficient mass to absorb the kinetic energy of the projectile and remain intact. The target will disintegrate. Thus, there are two factors that must determined before a prediction can be made as to what type of hypervelocity collision will occur. The depth to which the projectile can penetrate a target must be determined and then the mass of the target must be compared to the mass of the projectile.

4.1.3 Collision Type Specifications.

A thin plate collision occurs when:

1. The target thickness (W_t) is less than 1.5 times the distance the projectile can penetrate a semi-infinite target (P_t) and:

2. The mass of the target M_2 is at least 115 times greater than the mass of the projectile M_1; $M_2 > 115M_1$.

Or, if stated in a single conditional statement

$$W_t \leq 1.5 \, P_t \cap M_2 > 115M_1. \tag{19}$$

In a thin plate collision the projectile will be partially or totally destroyed and the target will be perforated, leaving a final hole diameter of up to a few times the projectile's diameter(16:106). The thinner the target, the less massive it must be to remain intact during the collision. This is because a given projectile will do work against thin targets for less time. Therefore, a *thin* thin plate target will not absorb as much energy as a *thick* thin plate target (see Figure 13).

30

A thick target collision occurs when:

1. The thickness of the target (W_t) is greater than 1.5 times the distance the projectile can penetrate a semi-infinite target (P_t) and:

2. The mass of the target M_2 is at least 115 times greater than the mass of the projectile M_1; $M_2 > 115M_1$.

Or, if stated in a single conditional statement

$$W_t > 1.5\,P_t \cap M_2 > 115M_1. \tag{20}$$

When a kinetic energy projectile hits a thick target, the projectile is stopped by the target and all of its energy is absorbed by the target and the resulting debris.

A small target collision occurs when:

1. The thickness of the target (W_t) is greater than 1.5 times the distance the projectile can penetrate a semi-infinite target (P_t) and:

2. The mass of the target M_2 less than 115 times greater than the mass of the projectile; M_1, $M_2 < 115M_1$.

Or, if stated in a single conditional statement

$$W_t > 1.5\,P_t \cap M_2 < 115M_1. \tag{21}$$

In a small target collision, the projectile is roughly the same size as the target, and a catastropic collision results because the structure of the target is not massive enough to absorb all the projectile's energy and remain intact. The entire target is destroyed and converted to debris. This type of collision should be avoided when conducting ASAT engagements because large chunks of debris are produced. This is because the target breaks apart before the projectile's energy is spent liquifying the target material. These large pieces of debris will stay in orbit longer, thus increasing the chance they will collide with a spacecraft, and if a collision does occur, the larger pieces will incur greater damage.

4.2 THIN PLATES

Consider a right circular cylinder, whose length is equal to its diameter, impacting a thin shield at hypervelocity. The estimated wave pattern shortly after impact is shown schematically in Figure 9. It is seen in (9a) that two shock waves, S_1 and S_2 have propagated away from the interface I, and because the projectile is finite in diameter, rarefaction waves R_1 and R_2 have been transmitted toward the axis of symmetry. Also, the formation of these rarefactions has resulted in the ejection of both projectile and shield material in a rearward direction. Now consider the situation shortly after the shock S_2 has reflected from the back face of the shield (9b). In order to satisfy the boundary condition of zero pressure, the shock is reflected as a rarefaction wave R_3. The resultant particle velocities behind R_3 are such that the profile of the back face of the shield is as shown in the figure. As the process continues, the bubble grows through the addition of material from the shield and projectile.(16:106-107)

From the description above, it can be seen that the debris generated in a rearward direction is that which is created *before the thin plate is perforated.* As soon as the plate is breached, the debris will travel in the same general direction as the projectile.

4.2.1   Total Mass of Debris Created in a Thin Plate Collision. To calculate the total mass of debris that is generated during a thin plate collision, one only needs to determine the size of the hole that will be created and multiply the volume of that hole (Vol_h) by the density of the target material (ρ_t). This is easier than it sounds because the size of the projectile launched is already known, and there is a good correlation between the radius of the projectile and the radius of the hole that it will create in a thin plate collision. The only unknowns are the density of the target material and the thickness of the target. The strength of the target material was found to be not significant for determining perforation radii (29:274).
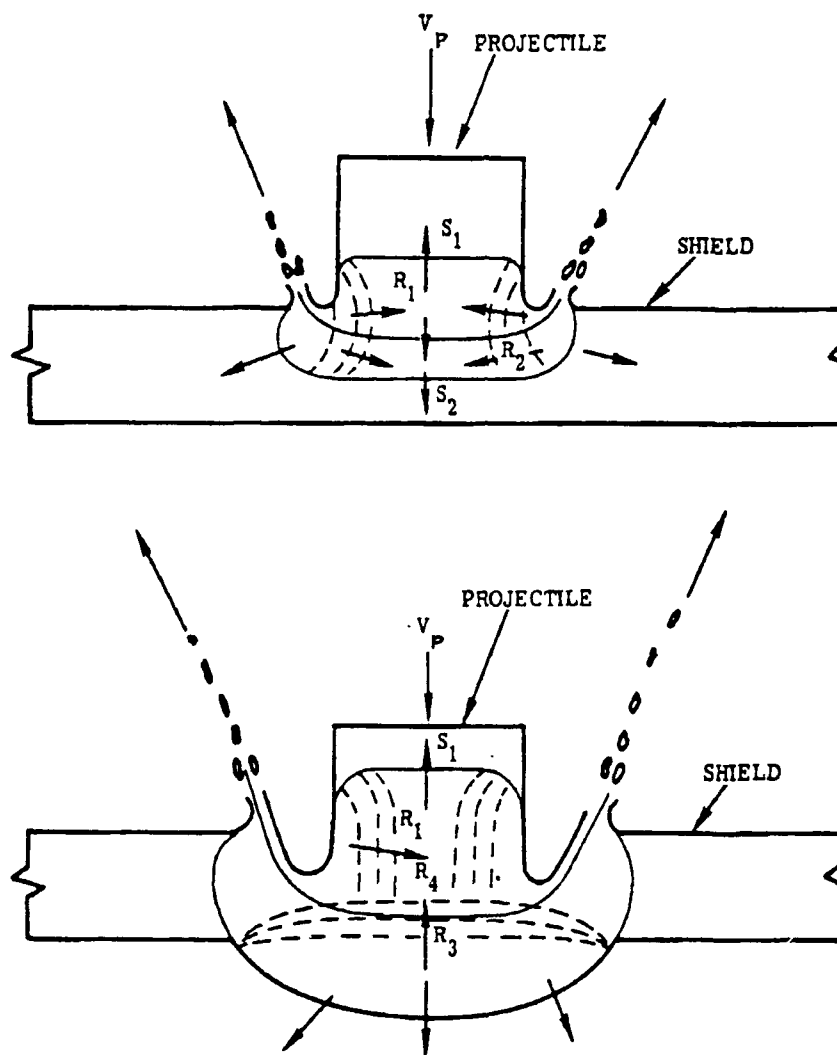
Figure 9. Estimated Wave Pattern. (a) In a projectile and shield soon after impact; (b) after reflection of shock from bottom face of shield.

(17:70)

33

5

4

$\dfrac{D}{d} = \dfrac{\text{Hole Dia.}}{\text{Proj. Dia.}}$

3

2

1

0

W_t/d

0.504

0.384

0.256

0.040

0   1   2   3   4   5   6   7   8   9

Projectile Impact Velocity (km/sec)
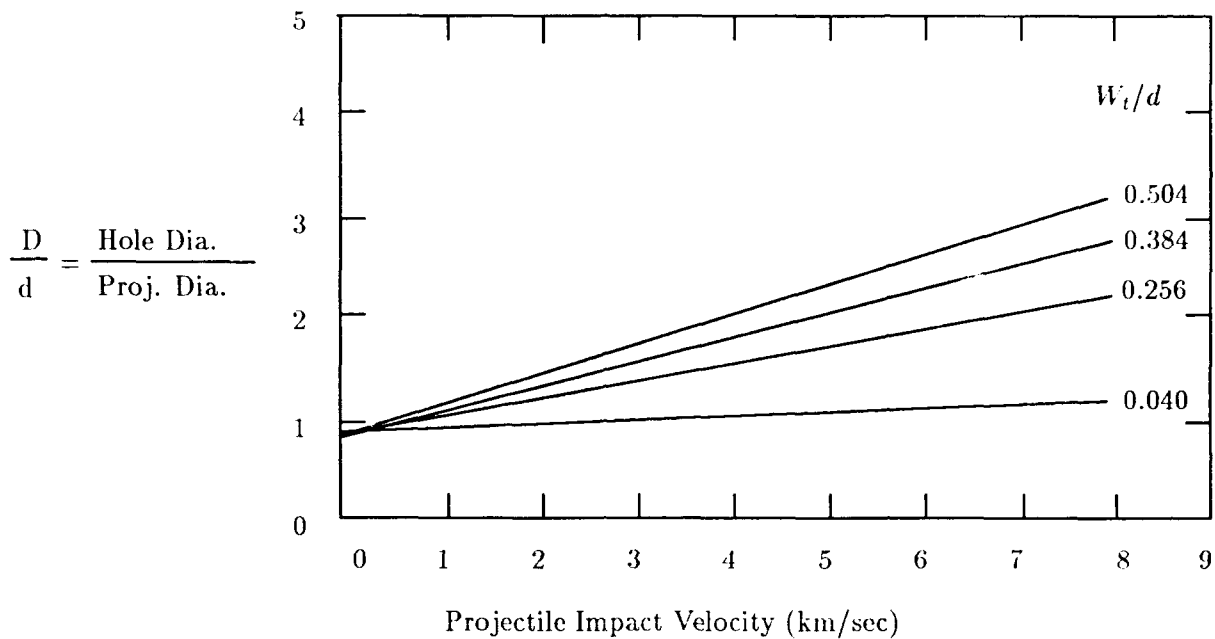
Figure 10. Hole Size in Shields for Aluminum Projectiles and Shields.
(16:117)

For the radius of the hole left by the projectile, refer to Figures 10 and 11. These figures will provide an estimation for the size of the hole, given the shape of the projectile and its radius are known. Figure 11 was generated from experiments where the mass of the projectile was held constant, and its shape was changed from a long rod to a coin shaped disk. It should be noted that although the radius of the hole created by the projectile increases as projectile radius increases, the depth the projectile penetrates the target is reduced.

For a more precise figure on the size of hole caused by a projectile perforating a thin plate, Gehring (16:117) found that for a specific shield thickness, the hole diameter is approximately a linear function of velocity. This relationship is quantified in the following equation.

$$D/d = 0.45\ V_p\ (W_t/d)^{2/3} + 0.90 \qquad (22)$$
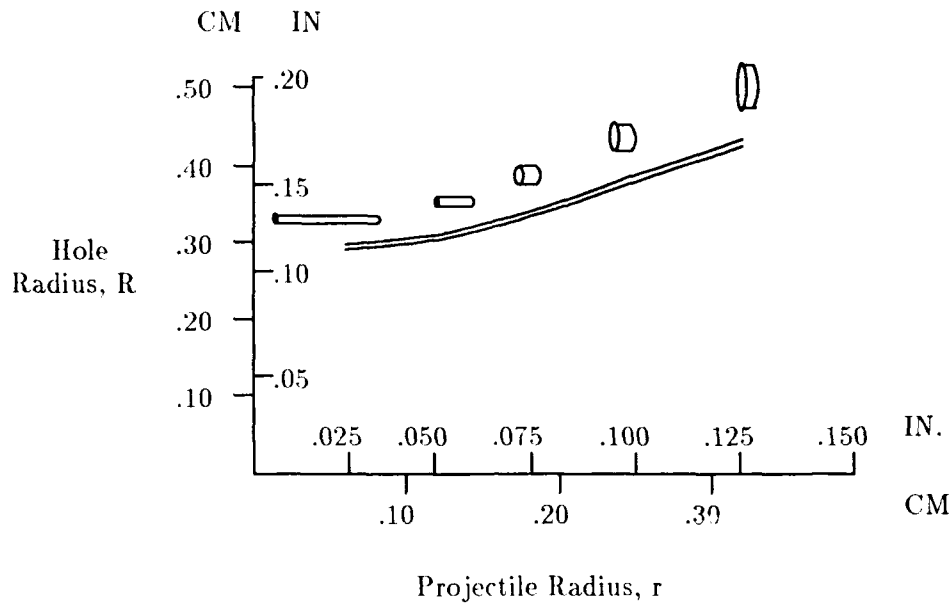
Figure 11. Radius of Perforation as a Function of Projectile Radius
(29:297)

For the notional projectile penetrating the 93 cm plate, this works out to be

$$D/d = 0.45 \times 10 \times (.93/.196)^{2/3} + 0.90 = 13.6 \qquad (23)$$

From the equation, the ratio of the hole diameter (D) to the projectile diameter is 13.6. The notional projectile has a radius of 9.8 cm, and since the ratio of the diameters is also the ratio of the radii, the hole formed in the thin plate target will have a radius of 9.8 × 13.6 = 133 cm (or less). Since hole diameter is a function of target thickness, a thinner target will have a smaller hole from the same projectile.

If the density of the target material cannot be determined, a good estimation for its density would be 2.78 g/cu. cm because this was calculated to be the average density of objects in earth orbit (30:79). As for the thickness of the target, it was determined in the previous section that the notional projectile can penetrate a thin plate target that is less than 93 cm thick. So, 0.93 meters can be used as a maximum figure for the thickness of a thin-plate target.

35

Thus, the maximum total mass of material ejected from a thin plate collision can be calculated.

$$M_c = \text{Vol}_h \rho_t \tag{24}$$

The volume of the hole can be closely approximated by the volume of a cylinder which is

$$\text{Vol}_h = \pi R^2 W_t \tag{25}$$

where:

R = radius of the hole

W_t = target thickness

Substituting in the values for the hole radius and target thickness produces the following result

$$\text{Vol}_h = \pi 1.33^2 (.92) = 5.11 \text{ cu. meters} \tag{26}$$

Now, multiplying the volume of the hole by the density of the target material will give the mass of debris produced in a thin plate collision:

$$5.11 \times 2,780 = 14,200 \text{ kg} \tag{27}$$

Thus, the notional projectiles is capable of producing a maximum of 14,200 kg of debris in a thin plate type collision. It should be noted that this is roughly five times the mass of debris that can be generated by the notional projectile colliding with a thick target.

4.2.2 The Number of Debris Particles Created in a Thin Plate Collision. To calculate the number of debris particles created during a collision between the notional projectile and a thin plate target, Kessler's Formula 7 will be used. This formula is only applicable to non-catastropic collisions such as thin plate and thick target collisions. It cannot be used to estimate the number of debris fragments generated in a small target collision because in a small target collision, the target may break up long before the projectile's kinetic energy is spent, thus making fewer but larger debris fragments than in the other two collision types.

36

The values for the constants (0.8 and -0.8) were found by conducting impact experiments, in a laboratory, on spacecraft structures (4:7).

$$N = 0.8(M/M_e)^{-0.8} \qquad (28)$$

where:

N = Number of ejected fragments with mass M and larger

M = Minimum mass of particles to be considered

M_e = Ejected debris mass

As stated in Chapter One, only particles with diameters greater than one centimeter will be considered in this effort. To determine the mass of such a minimum particle, its volume is multiplied by the density of the target material.

Minimum particles mass:

$$M = 4/3\,\pi\,r^3 \times \text{ (density of target)} \qquad (29)$$

For a particle radius of .5 cm and a target density of 2.71 g/cu. cm, the equation looks like:

$$M = 4/3\,\pi\,.5^3 \times (2.71) = 1.41\,\text{grams} \qquad (30)$$

Thus, the minimum mass of debris particles to be considered by this effort will be 1.41 grams. By substituting this value and the value for the total mass of debris created in a thin plate collision (Equation 27), the number of fragments, larger than 1 cm in diameter, that will be produced can be calculated.

$$N = 0.8(.00141/14,200)^{-0.8} = 320,000 \qquad (31)$$

So, when the notional projectile collides with a thin plate target, a maximum of 320,000 pieces of debris, with diameters greater than one centimeter, will be produced. Less debris will be generated by thinner targets.
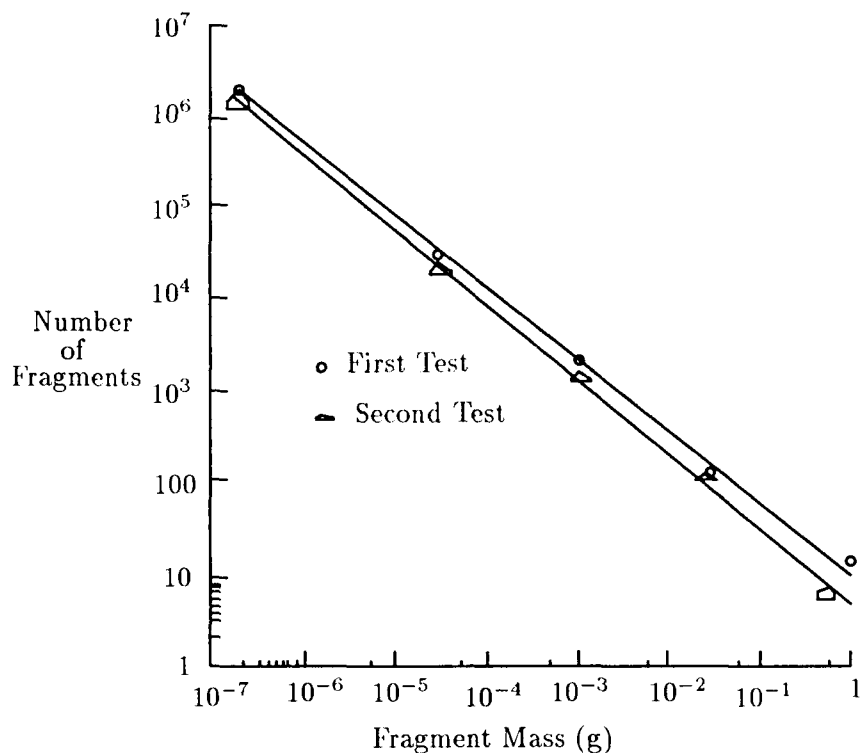
Figure 12.   Cumulative Fragment Mass Distribution From Meteoroid Impact of Spacecraft
Wall.

(4:25)

4.2.3   Mass Distribution of Debris Created in a Thin Plate Collision. In 1972,
Dynamic Response of Materials was published in which H. F. Swift wrote an appendix,
including the following quote.

Perhaps the most important new area of interest is the study of projectile
and target fragmentation during hypervelocity impact of thin plates. The size
distribution of solid fragments in debris clouds is the most important single pa-
rameter controlling cloud lethality to vehicle structures. To date, almost noth-
ing is known about these size distributions or the material shattering processes
that produce them; and, no quantitative results relating such distributions to
cloud damage potential are available. (6:535)

In 1975, T. D. Bess published a NASA Technical Note, *Mass Distribution of Orbiting Man-Made Space Debris*, which described work done to determine this "most important single parameter controlling cloud lethality to vehicle structures." To determine the mass distribution of debris fragments from a hypervelocity impact, Bess fired hypervelocity projectiles into a "simulated spacecraft," then sorted and weighed the resulting debris The results of the experiment are summarized in Figure 12. The graph shows that many small pieces of debris were produced (1,000,000 pieces with mass 10^{-7} g) and very few large pieces (about 10 pieces with a mass of one gram).

4.2.4 Velocity of Debris Created in a Thin Plate Collision. As it was noted in the literature review that there is some disagreement in the velocity of debris particles created in a hypervelocity impact. Bess (4:1) states, "Velocities of fragments resulting from hypervelocity impact were on the order of 10 meters per second..." Whereas Cintala (5:581) states, "This jetted mass is rapidly accelerated to velocities well in excess of the impact velocity..."(10 km/sec).

Bess' experiment involved hitting a "simulated spacecraft" with two small projectiles (1.65 grams and 0.37 grams) at 3 and 4.5 km/sec respectively *in earth normal atmosphere* (the tests were conducted outdoors). Because of its small mass, it is likely the molten ejecta from the tests was decelerated quickly as a result of air drag.

This hypothesis is support by Bess' description of the ejecta as "irregularly shaped, flat plates." Other literature suggests ejecta from a hypervelocity collision is composed largely of spheres that have coalesced from molten projectile and target materials. If these rapidly moving molten spheres are traveling through air, it is likely they will be flattened and cooled, resulting in the shapes described by Bess. These flattened spheres will be very un-aerodynamic and slow quickly. It is for these reasons that Bess' figures on ejecta velocity will be disregarded for this effort. All of the collisions modeled herein are assumed to be in space, where the spherical debris fragments will not be slowed and deformed by the atmosphere.
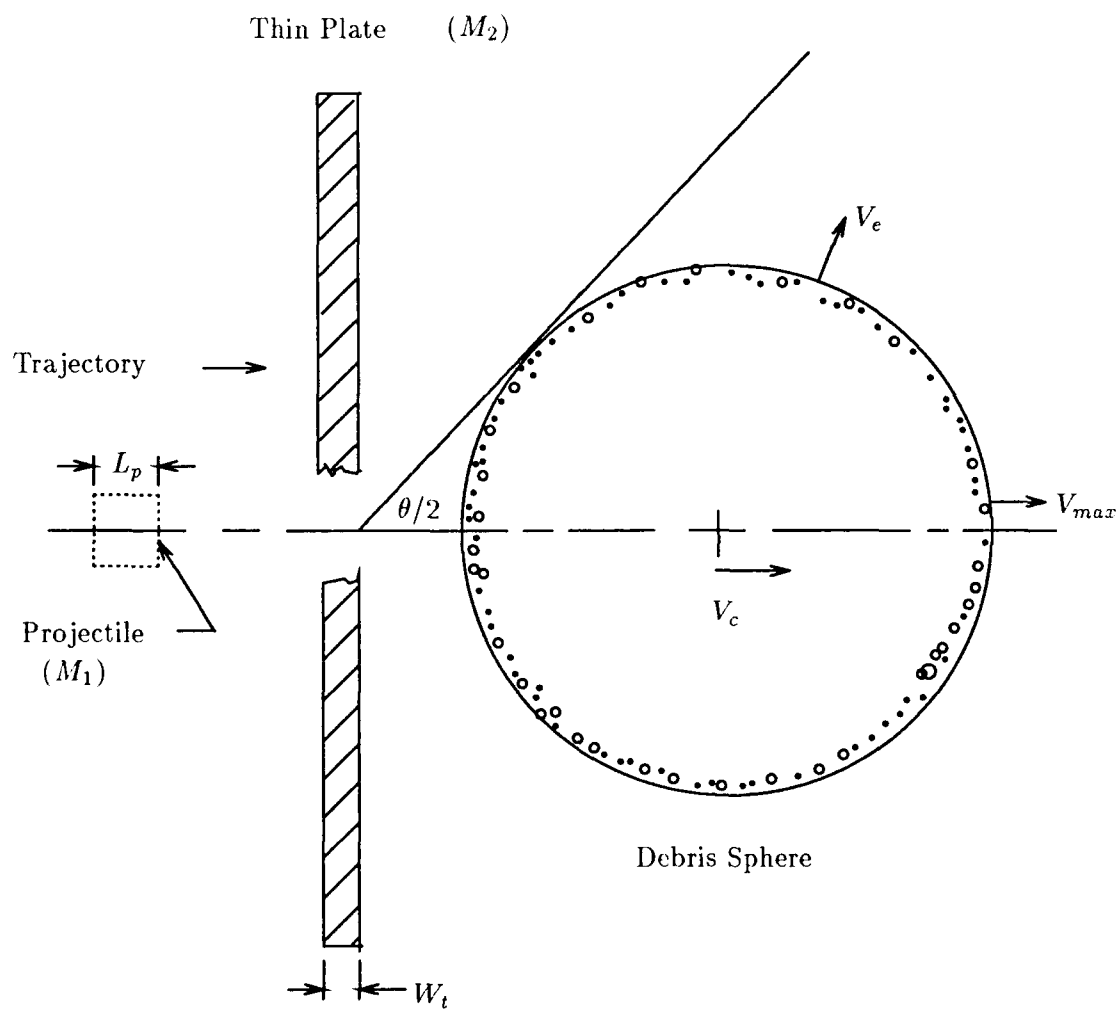
Figure 13. Forward-Moving Debris Cloud From a Thin Plate Collision
(35:227)

The following two sections provide models for calculating the velocity of debris resulting from a thin plate collision

4.2.4.1 Debris Sphere Velocity Model.

In *Hypervelocity Impact Mechanics* H. F. Swift models the debris exiting the rear of a thin plate collision as an expanding sphere where, "All of the materials within the sphere are assumed to be concentrated at its surface which corresponds accurately to a wide range of experimental observations."

Referring to Figure 13, Swift provides the following equations for V_c, the velocity at which the center of the sphere is moving; V_e, the velocity the edge of sphere is moving away from its center; and V_{max}, which is the velocity the forward edge of the sphere.

$$V_c = V_p/(1 + KG^2) \tag{32}$$

V_p is the velocity of the projectile, K is the ratio of the masses per unit area of the projectile and the target plate, and G is the ratio of projectile diameter to the target that contributes debris to the spherically expanding cloud.

An expression for the outward velocity of the debris cloud from its center of mass is:

$$V_e = V_p G[\sqrt{QK}/(1 + KG^2)] \tag{33}$$

In this equation, Q is the fixed fraction of energy appearing as directed kinetic energy. It is also described as "the ratio of kinetic energy to heat energy in material of the debris cloud" and "fraction of energy available to debris-cloud formation expended or directed kinetic energy." Unfortunately, Swift doesn't provide any further explanation or values for the constant Q. However, it sounds very much like the value for E_s calculated in Section 4.3.1.1. E_s is defined as the thermal and kinetic energy of spray material which leaves the target. In that section, E_s was found to be 0.345 times the kinetic energy of the projectile (E_p). Thus, the ratio $E_s/E_p = 0.345$. For the purposes of future calculations, it will be assumed that $Q = E_s = 0.345$.

As can be seen from Figure 13, V_{max} is the sum of V_c and V_e or:

$$V_{max} = V_p[(1 = G\sqrt{QK})/(1 + KG^2)] \tag{34}$$

"The angles subtended at (the) original impact site, by the opposite edges of the cloud may now be calculated since the sine of the half-angle, $\theta/2$, is simply the ratio of the cloud expansion velocity, V_e, to the velocity of the clouds center of mass, V_c" (35:228).

$$\theta/2 = \arcsin\sqrt{QK} \tag{35}$$

4.2.4.2 Debris Cone Velocity Model. Another model for the velocity of debris resulting from a thin plate collision was provided by B. J. Henderson et al., in their report "Very High Velocity Penetration Model." Rather than an expanding sphere, the debris in Henderson's model is described as forming a cone with its vertex at the collision site:

$$V_x/V_y = d(0.01 \times V_o + 0.127) \tag{36}$$

where:

V_x = Velocity (km/s) Parallel to Target Plate (Perpendicular to V_o)

V_y = Velocity (km/s) Perpendicular to Target Plate (Parallel to V_o)

V_o = Initial Velocity Vector of Projectile (km/s)

d = Projectile Diameter (cm)

As in Swift's sphere model, the half-angle of the debris cone can be calculated using the ratio of velocities.

$$\theta/2 = \arctan d(0.01 \times V_o + 0.127) \tag{37}$$

For the notional projectile, the equation is

$$\theta/2 = \arctan 19.6(0.01 \times 10.0 + 0.127) = 77.3 \, \text{deg} \tag{38}$$

This value seems too large. From the equation, the ratio of debris velocity perpendicuular to the projectile's trajectory to the debris velocity parellel to the projectile's trajectory works out to be 4.43. This contradicts experimental data obtained by the Air Force Materi s Lab that shows debris velocity from a thin plate collision being the greatest along the projectile's trajectory and falling off as the angle from that trajectory increases (see Figure 14). There seems to be a problem with this equation, because it does not take into account target thickness. The equation suggests that debris dispersion angle is dependent solely on the projectile's velocity and diameter and that target thickness is not a consideration. Target thickness is considered in Swift's model and would seem to play a significant role in determining debris spray angle. Perhaps Henderson was using this equation for a particul.r target thickness, and that is how the constants where derived. Unfortunately, the conditions for the use of this equation are not specified in the report, and the approach taken here does not seem to give a valid figure for debris velocity. As a result this equation will not be used further.
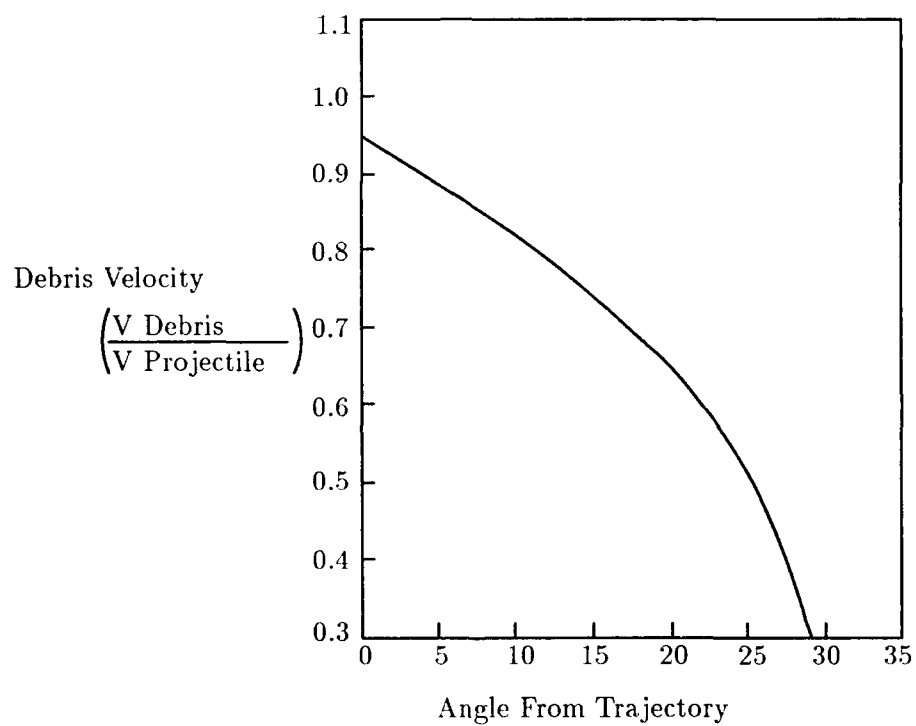
Figure 14. Velocity of Debris Fragments as a Function of Angle From Projectile Trajectory.

(6:532)

4.2.5 Target Spalling. Another phenomenon that should be considered when estimating debris production in hypervelocity impacts is called *spalling*. Spalling can be defined as fracture resulting from reflection of a decaying shock wave from a free surface (16:472).

> When a particle strikes a plate at high velocity, it forms a crater in the front surface of the plate and starts a strong compressive shock. This shock, attenuated as it travels through the plate, is generally reflected off the rear surface (or any free surface) as a tension wave. If the plate is thin enough, or if the initial shock is strong enough, the reflected tension wave will be so intense that a portion of the free surface of the plate may be ejected with a momentum sufficient to damage other parts of the structure...The diameter of the spall is usually two or three times the thickness of the plate; the thickness of the spall is usually in the range of $\frac{1}{10}$ to $\frac{1}{2}$ the thickness of the plate (16:472).

What this means is that in a collision with a flat plate, even though the projectile may not penetrate the plate, target material may be ejected from the rear of the plate, if the projectile imparts sufficient energy. Thus, for a narrow range of projectile energies and target thicknesses, debris will be generated from both sides of an unperforated flat plate.

The volume of debris generated can be estimated by using the thick-target calculations for the side of the plate impacted by the projectile, and the thickness of the spall can be estimated by the following equation (16:472):

$$t = (\rho_c/\rho_o)(\lambda/2) \tag{39}$$

where t is the spall thickness, ρ_c is the critical stress necessary to fracture the material, ρ_o is the maximum stress in the compressive wave, and λ is the length of the pulse.

Unfortunately, the above equation can only be used as an estimate because, "The calculation of spall thickness and velocity is difficult because neither the magnitude nor the shape of the compressive pulse are well-defined for given conditions of impact" (16:472).

However, as Figure 16 shows, the portion of target thickness over which spalling can occur is relatively small, so spalling won't be a major factor in debris production. But, it is a debris source that should be considered.
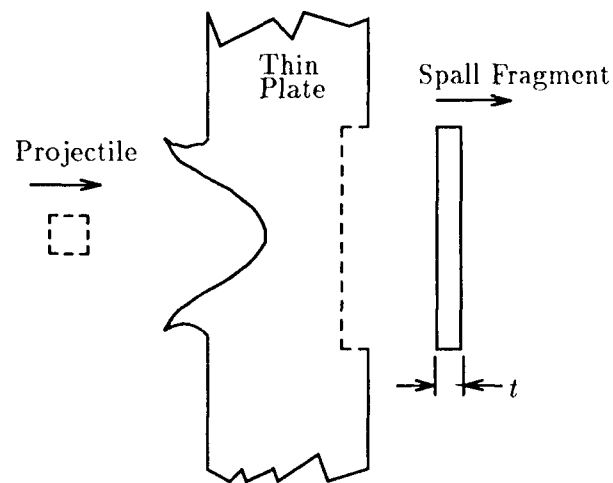
Figure 15. Spall Formation in a Target of Intermediate Thickness
(35:221)

Thickness of Target (W_t)
―――――――――――――――
Diameter of Projectile (D_p)
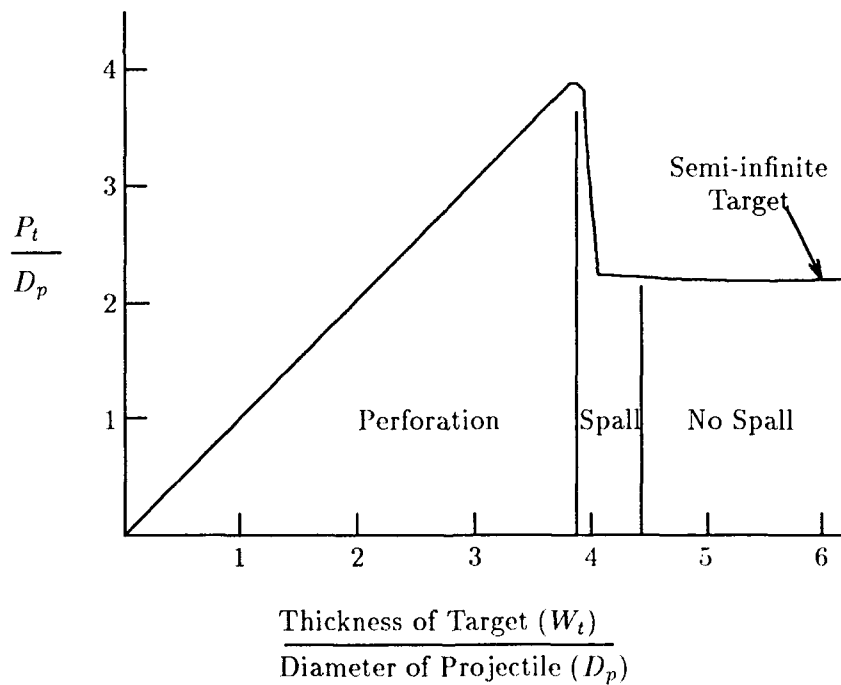
Figure 16.   Depth of Penetration (P_t) Versus Target Thickness-Flat Targets. Targets: 2024-T3 Al. Projectiles: 3.18-mm 2017 Al spheres, 0.047 g. Velocity: 7.4 km/s.

(16:475)
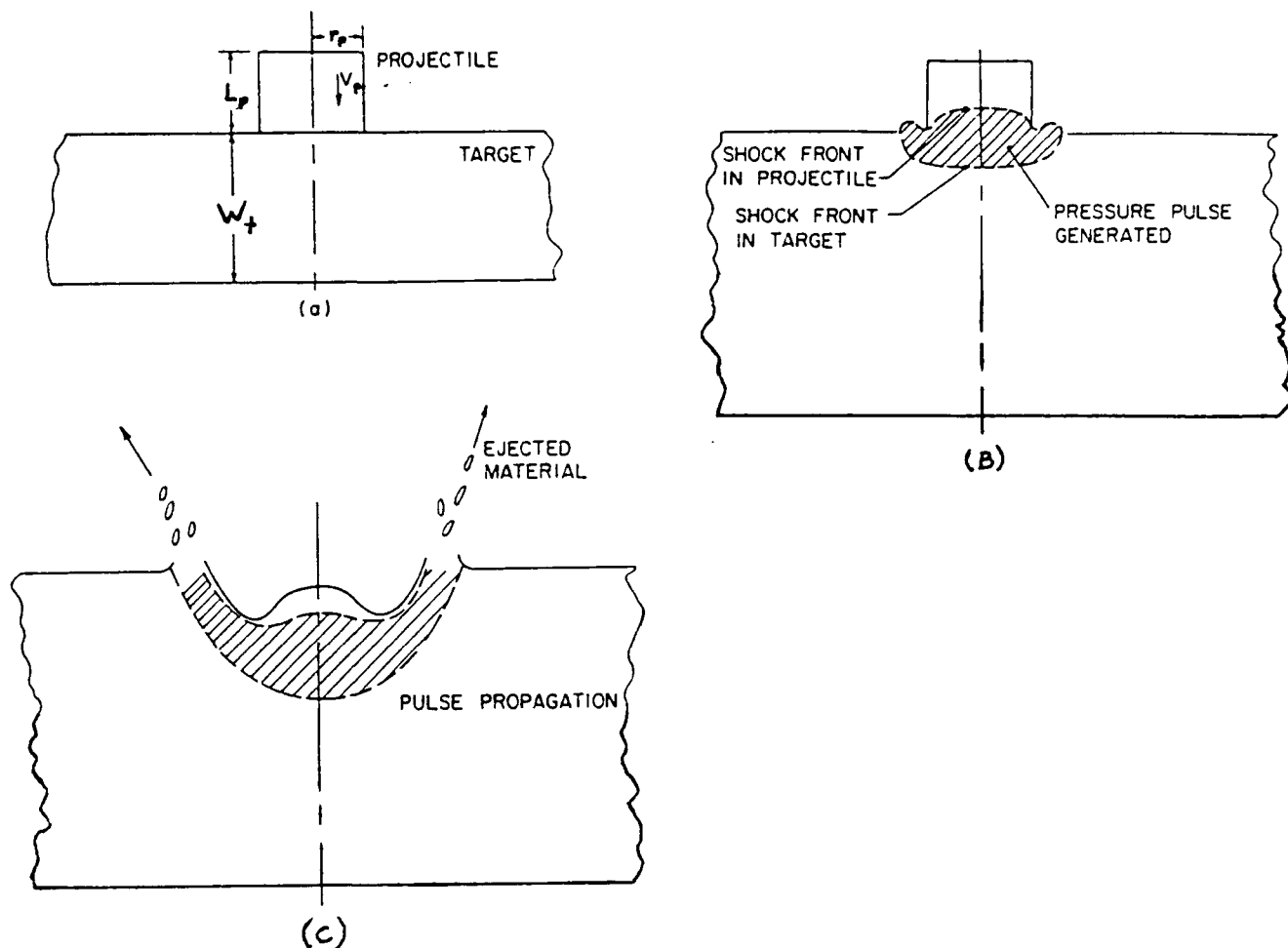
Figure 17. Thick Target
(22:88)

4.3 THICK TARGETS

In the very earliest stages of the event, as the projectile makes contact with the target, two shock waves are formed; one travels into the target, while the other moves back into the projectile. The combination of high shock pressures (typically on the order of hundreds of kilobars to megabars for the events considered important here) and free surfaces yield violent decompression and high-velocity ejection of molten and vaporized material, giving rise to a hydrodynamic process generally referred to as "jetting" (Gault et al. 1968)...By the time the shock wave reaches the trailing end of the projectile, the majority of the transferral of energy to the target is complete. The time elapsed from initial contact to this stage in the event is on the order of the time taken for the shock wave to traverse the length of the projectile. (5:580)

4.3.1   Total Mass of Debris Created in a Thick Target Collision. There are several equations available for calculating the mass of debris that results from a collision with a thick target. In this section, three different approaches will be taken to determine the actual mass. The first method estimates the fraction of projectile energy used in creating debris, and using figures already available on how much energy is required to produce a given mass of debris, calculates the total mass of debris that can be produced. The second method uses equations which calculate the volume of the crater produced in a collision, then multiplying the density of the target material times the crater volume gives the mass of debris produced. The last method is to use equations already created by other sources which directly calculate the mass of debris which will be produced in a given collision. By using three different methods, it is hoped that a good figure for the mass of debris produced in a thick target collision can be produced.

4.3.1.1   Energy Partitioning in Cratering. To analyze the dynamics of a projectile colliding with a thick target, it will be useful to first determine how the projectile's kinetic energy is distributed in the target. That is, how much energy goes into causing heating of the target? How much energy is used in creating debris and how much is used in the movement of materials within the target?

According to E.P. Palmer and G. H. Turner (21:18), the energy balance can be described in the following way:

$$E_k = E_h + E_s + E_r \qquad (40)$$

where:

E_k is the kinetic energy of the projectile,

E_h is the heat energy appearing in the target due to irreversable deformation and shock heating and the degradation of sound waves into heat,

E_s is the thermal and kinetic energy of spray material which leaves the target (this partition is of primary importance for this study), and

E_r is the energy of recrystallation and strain in the target material.
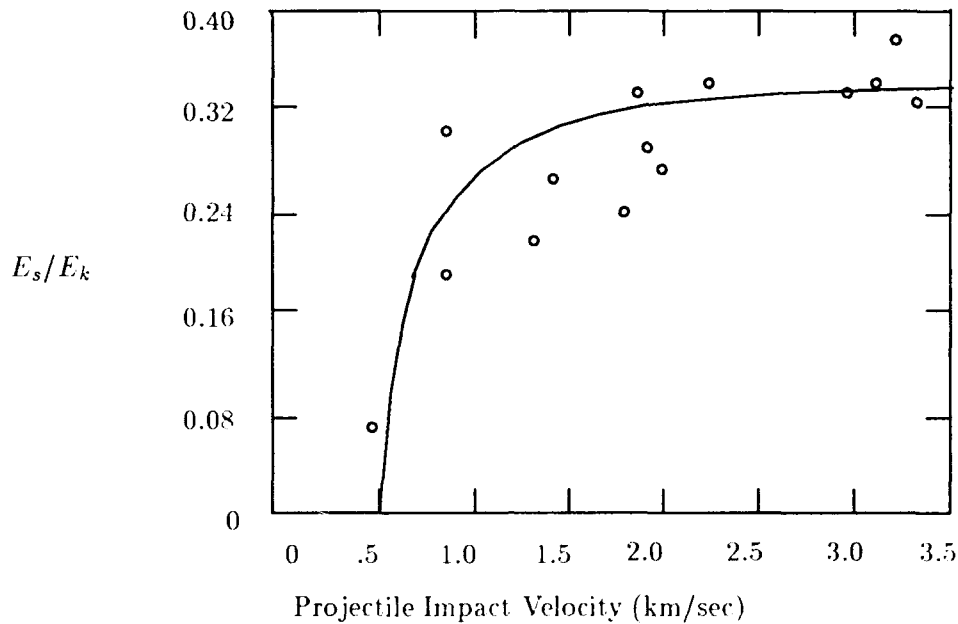
Figure 18.   The Fraction of Kinetic Energy of the Projectile Appearing as Spray Particle
Energy, E_s/E_k, Plotted as a Function of the Impact Velocity
(21:18)

For the purposes of this effort, it is important to know what fraction of the total energy is used in producing debris. According to the study by Palmer, the fraction of energy used in creating debris is a linear function of the projectile's kinetic energy when the projectile is traveling greater than 3.5 km/s. It turns out that about one-third (34.5%) of the projectile's energy is used in creating and heating debris particles (see Figure 18).

Unfortunately, the proportion of energy used in heating the debris is not given. However, the energy partitioning experiments listed above can be used to determine an absolute upper bound of debris mass that can be produced. By assuming that no energy is used in heating the debris and that all of it is used up in creating debris, one can derive a theoretical upper limit on the mass of debris that can be created by a particular projectile. For the 16 kg notional projectile, moving at 10 km/s, its total kinetic energy is 800 Mjoules $(1/2 \times 16 \times 10,000^2)$. Multiplying by the fraction of the projectile's kinetic energy used in creating and heating debris $(E_s = 0.345 \times 800$ Mjoules) gives 276 Mjoules of energy.

49

From laboratory experiments conducted by E.P. Palmer and G. H. Turner (21:18), in which they make energy measurements using 3/16-inch diameter chrome-steel balls fired into lead targets, it was determined that 114 joules yields one gram of debris (or 114,000 joules/kg). If it is assumed that it takes about the same magnitude of energy to create debris from satellite materials, and it is furthur assumed that all of the energy is used in creating debris and none is spent heating the debris (not a valid assumption), and then dividing E_s by 114, the maximum possible mass of debris produced can be calculated. For our notional projectile this yields:

$$2.76 \times 10^8 \, \text{J}/114,000 \, \text{J/kg} = 2,420 \, \text{kg} \tag{41}$$

4.3.1.2 Volume Method for Estimating Debris Mass. In *Impacts Dynamics*, Swift states, "Another interesting feature of these craters (produced in thick targets by hypervelocity projectiles) is that the crater volume, V_c, per-unit kinetic energy of the projectile, E_p, is nearly constant for each combination of projectile material and target material."

$$V_c = K \, E_p \tag{42}$$

By multiplying both sides of the above equation by the density of the target material, the mass of debris produced in the collision can be calculated.

$$M_c = K \, E_p \, \rho_T \tag{43}$$

According to Swift (35:219), the constant K ranges in value from $.5 \times 10^{-10}$ to 2.0×10^{-10} cu. cm/erg. Without knowing the value of K for our target material, upper and lower bounds on the amount of mass ejected can be predicted.

From the table, the estimation of debris mass ranges from a low of 1,110 kg to a high of 4,450 kg. This range accounts for many differnt types of material that might be excavated from the impact crater. The volume of the crater changes and is dependent on the density of the particular target material. Each value for K indicates how much energy is required to excavate a given volume of the target material. Higher values of K indicate that more material is removed per unit of energy.

	Minimum and Maximum Debris Mass	

$$M_e = K\, E_p\, \rho_T$$

Minimum Debris Mass	Maximum Debris Mass
$K = .5 \times 10^{-10}$ cc/erg	$K = 2.0 \times 10^{-10}$ cc/erg
$M_e = .5 \times 10^{-10}(8.0 \times 10^{15})(2.78)$	$M_e = 2.0 \times 10^{-10}(8.0 \times 10^{15})(2.78)$

$M_e = 1.11 \times 10^{6}$ grams (1,110 kg)	$M_e = 4.45 \times 10^{6}$ grams (4,450 kg)

Table 3. Volume Method for Debris Mass Calculation

The values of M_e given by the this method (1,110 - 4,450 kg) nicely bracket the value given by the energy partitioning method in the previous section (2,420 kg).

4.3.1.3 Canned Formulae. This next section uses two formulas, found in the literature, which calculate debris mass directly. Kessler's Formula 4 will be used first.

$$M_e = 115 \times 16\,\text{kg} \tag{44}$$

Kessler's formula predicts that 1,840 kg of debris will be created in our notional attack against a thick target. Which is consistant with the preveious results because 1,840 is close to the 2,420 kg value predicted by the energy partitioning method, and is also between the extremes predicted in the volume method.

Lastly, Moore's Formula 45 will be used to calculate the debris mass:

$$M_e = 10^{-10.613}[(\rho_p/\rho_t)^{1/2} \, E_p]^{1.189} \tag{45}$$

where:

M_e = Ejected mass

E_p = Projectile energy = 800 Mjoules (8.0 × 10^{15} ergs)

ρ_p = Projectile density = 2.71 g/cu. cm

ρ_t = Target density = 2.85 g/cu. cm

Substituting in the values above:

$$M_e = 10^{-10.613}[(2.71/2.85)^{1/2} \, 8.0 \times 10^{15}]^{1.189} = 1.918 \times 10^8 \, \text{grams}(192,000\text{kg}) \tag{46}$$

This value is about 50 times as large as any other calculated value and is about 50 times the mass of the target, so it will be disregarded. Moore's formula does not seem to be valid for hypervelocity impacts involving large projectiles.

The three valid methods used to determine the mass of debris produced in a thick target collision gave the following results:

Energy partition: $M_e < 2,420$ kg

Volume method: $1,110$ kg $< M_e < 4,450$ kg

Canned Formula: $M_e = 1,840$ kg

From the above figures, a value of 2,400 kg will be used as a figure for the amount of debris produced in a thick target collision by the notional projectile.

4.3.2   The Number of Particles Created in a Thick Target Collision. To calculate the number of debris particles created during a collision between the notional projectile and a thick target, Kessler's Formula 7 will be used again.

$$N = 0.8(M/M_e)^{-0.8} \tag{47}$$

As stated in Chapter One, only particles with diameters larger than one centimeter will be considered in this effort. In the thin plate section, the mass of such a particle was determined to be 1.41 g. By substituting this value and the value for the total mass of debris created in a thick target collision, we can calculate the number of fragments that will be produced:

$$N = 0.8(.00141/2,400)^{-0.8} = 77,200 \tag{48}$$

4.3.3 Mass Distribution of Debris Created in a Thick Target Collision. If the total mass of debris is divided by the number of debris particles (greater than 1 cm in diameter) created, the mean mass of the particles (ψ) can be obtained. This assumes the total mass of particles less than 1 cm is zero:

$$\psi = 2,400/77,200 = .0311\,\text{kg}(31.1\,\text{g}) \tag{49}$$

This is only a mathematical construct, as the mass of debris is not is not uniform, but follows the mass distribution shown in Figure 12. However, it can be useful in getting a general idea of the size of debris particles that result from a given collision. It can also be useful in comparing debris from one collision to that of another.

4.4 SMALL TARGETS

This section will describe what happens when a large projectile impacts a large target or when a small projectile impacts a small target. The key here is that the target and projectile are roughly the same mass (within a factor of 115) and that the target is thick enough to stop the projectile. It should be noted that if the projectile is more than 115 times more massive then the target, in essence, the projectile could than be thought of as "the target" and a small target collision won't occur. In this event, the target will be partially or totally destroyed and the damage to the projectile can be estimated using the thick target or thin plate models. Whether the projectile is closing on the target or vice versa, it is the closing velocities and relative masses of the bodies involved that determine the outcome of the collision.

4.4.1 Total Mass of Debris Created in a Small Target Collision.

In a small target collision, both the projectile and target are converted to debris. Expressed mathematically, the relationship looks like

$$M_e = M_1 + M_2. \tag{50}$$

Using the 16 kg notional projectile as an example, for a small target collision to occur, the target must be less than 1,840 kg and more than 140 g. Using the larger extreme, the total mass of debris that can be generated by the notional projectile, in this type of collision, is 1,856 kg.

Projectile

Target at
Start of Collision

Target and Projectile
Disintegrate
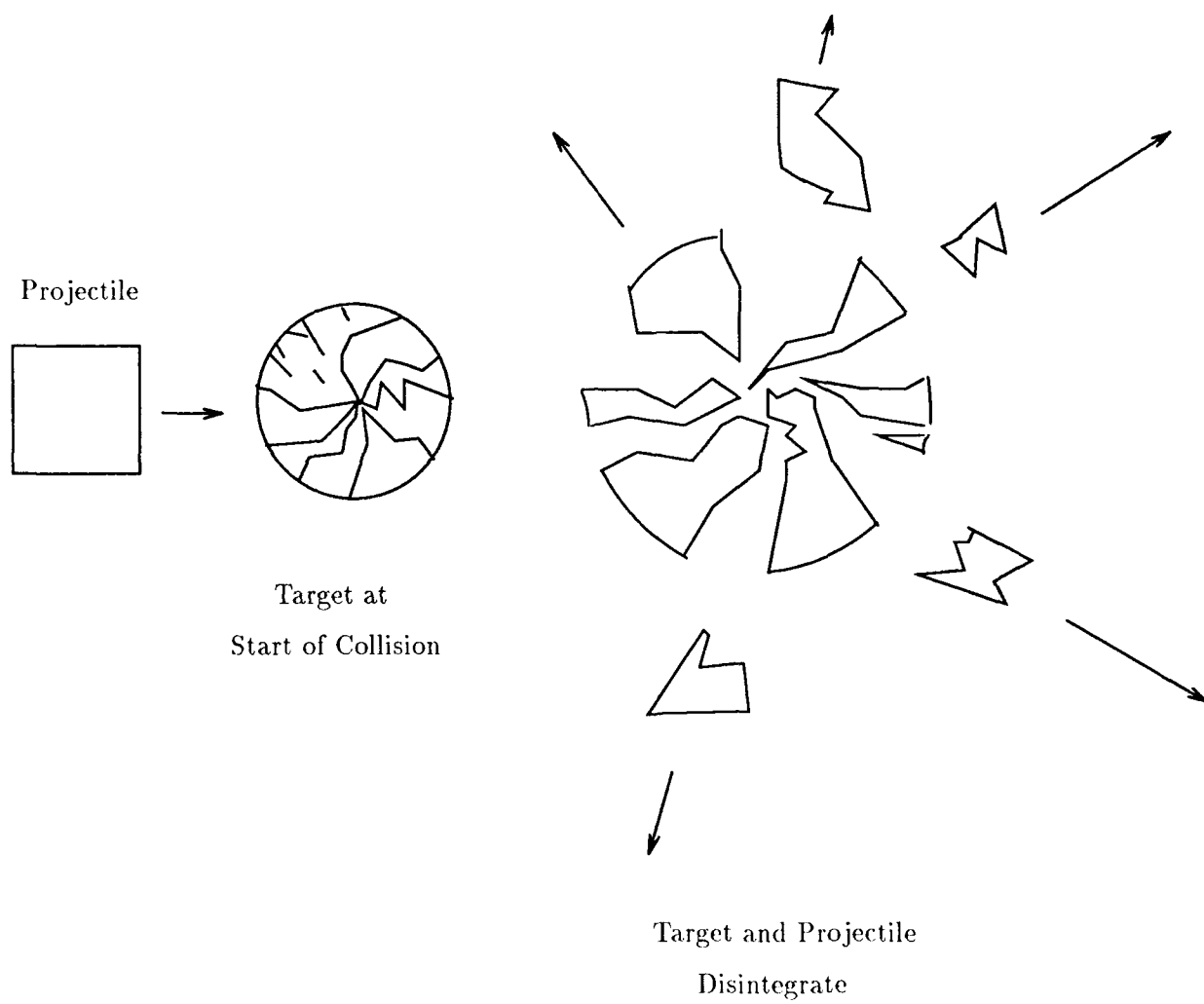
Figure 19. Small Target Collision

V. Satellite Engagements

5.1 THE NOTIONAL ATTACK

There are two basic collision orientations that are possible between the notional target and the notional projectile. These two possibilities are the end-on or side attack (see Figure 20).

END-ON ENGAGEMENT

Notional Projectile   Notional Target

SIDE-SHOT ENGAGEMENT
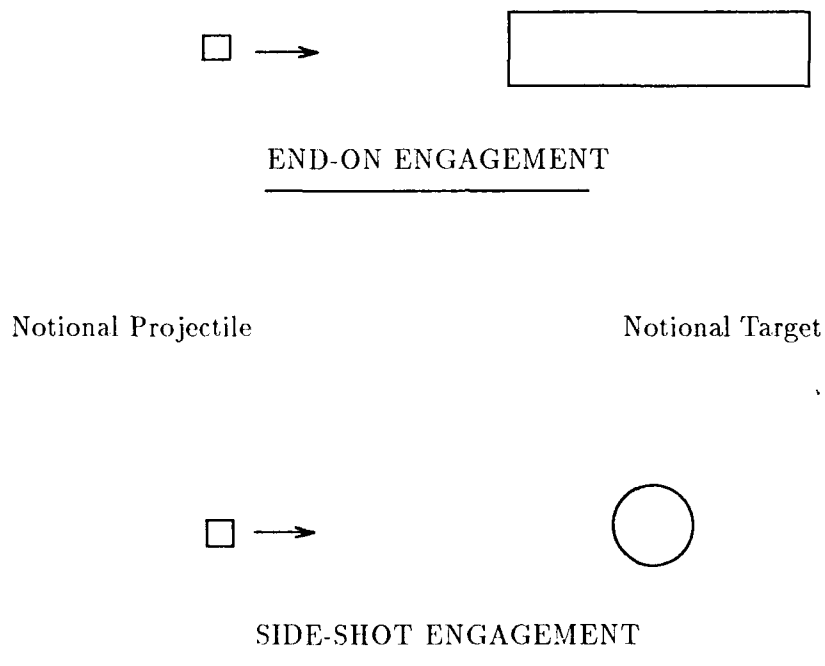
Figure 20. Notional ASAT Engagement Orientations

The end-on collision will occur when the projectile's trajectory coincides with the target's longitudinal axis. The side attack occurs when the projectile's trajectory is normal to the longitudinal axis. Of course, the angle of attack may vary from the two possibilities listed above, however, they serve as a good basis for illustration.

If the projectile collides with a surface of the target at other than 90 degrees, the penetration of the target can be estimated by using the component of the projectile's velocity which is normal to the surface (6:519). In such a case, the crater produced will take on an oval shape, and will not be as deep as in a collision with an equivalent projectile whose trajectory is normal to the surface.

The first step in predicting the result of an ASAT engagement is to determine which of the three types of hypervelocity collisions will occur. To do this, the distance the projectile can penetrate the target must be calculated and the mass of the projectile must be compared to the mass of the target.

In Chapter IV it was determined that the notional projectile, traveling at 10 km/s, can penetrate a semi-infinite aluminum target to a depth of 62 cm. The projectile to target mass ratio is $4,000/16 = 250$. Since the mass ratio is greater than 115 a small target collision cannot occur. The two choices remaining are a thick target or a thin plate collision. To differentiate between these two choices, the penetration depth must be compared to the targets thickness. Of course, the target's thickness in the notional attack depends on which of the two collision orientations is being considered. If an end-on collision occurs, the target's thickness will be 3.4 meters (the length of the notional projectile). If a side-shot collision occurs, the target thickness will be only 0.74 meters.

For the notional projectile, the dividing line between thick and thin targets was found in Chapter IV to be 93.0 cm (62×1.5). Thus, the end-on collision will most resemble a thick target collision and the side-shot collision will most resemble a thin plate collision.

5.1.1   End-on Attack. When the notional projectile collides with the end of the notional target, the projectile will penetrate the target until it expends all of its energy. The target will stop the projectile. If the target where semi-infinite in all dimensions, the projectile's penetration would be closely approximated at 62 cm. But, the target is only semi-infinite in depth (3.4 meters), not in width (74 cm).

According to Swift (35:216), the diameter of a typical hypervelocity crater, at the surface of the target, is approximately twice the penetration depth. This means the target would have to be at least 1.3 meters in diameter for a normal hypervelocity impact crater to form (in reality, it would probably have to be even larger due to the problem of rarefaction waves reflecting from the edges of the target and adding to the strength of the shock wave). This means the projectile will probably penetrate the target deeper than the 62 cm calculated for a semi-infinite target. In a thin plate target, where the shock waves from the collision reflect off of the far wall of the target and become involved in crater formation, the projectile can penetrate 1.5 times its penetration distance in a semi-infinite target(P_t). In the end-on collision, the rarefaction waves reflecting off of the sidewalls will reinforce the initial shock wave, causing more damage than what would be expected in an equivalent large target collision. Because a similar effect in thin target collision causes projectiles to penetrate more deeply, it seems reasonable to assume the projectile in the end-on collision will also penetrate a distance of about 1.5 × P_t. In this case, however, the reflected shock waves involved in crater formation will come from the side walls and not the surface at the opposite end of the target.

So, the notional projectile will penetrate the target to a distance of about 0.93 meters. Using this figure, the volume of target converted to debris can be calculated. Since the target is a cylinder, the volume of the target which is destroyed can be estimate by $Vol = \pi\, r^2\, h$. In this case penetration depth will be the height of the cylinder. So, the volume of target destroyed will be

$$\pi\, (.74/2)^2\, 0.93 \;=\; 0.40 \text{ cubic meters.} \tag{51}$$

Multiplying the target density (2,710 kg/cu. m) by the volume will give a good approximation of the mass of debris created in the end-on collision orientation ($2,710 \times 0.40 = 1,084$). In this type of collision about 1,100 kg of debris will be produced. This is only an approximation as no laboratory experiments were found in the research where hypervelocity projectiles were fired into the end of metallic cylinders. However, 1,100

kilograms of debris is consistent with the figure of 1,110 kg found in Section 4.3.1.2 using constants relating the amount of energy required to produce a given mass of debris.

To calculate the number of debris particles which will result, Formula 7 will be used:

$$N = 0.8(M/M_e)^{-0.8} \tag{52}$$

where:

N = Number of ejected fragments with mass M and larger

M = Minimum mass of particles to be considered (1.41 gram)

M_e = Ejected debris mass (1,100 kg)

Plugging in the above values gives

$$N = 0.8(.00141/1,100)^{-0.8} = 41,400. \tag{53}$$

The mass distribution in the debris particles should be similar to that shown in Figure 12, however, the mean mass of the particles will probably be larger.

Bess' tests:

First test: M_e = 13.85 grams

$N = 0.8(1.41/13.85)^{-0.8} = 5.0$

$\psi = 13.85/5 = 2.77$ g/particle

Second test: M_e = 8.20 grams

$N = 0.8(1.41/8.2)^{-0.8} = 3.27$

$\psi = 8.2/3.27 = 2.5$ g/particle

Notional Attack:

$\psi = 1,100/41,400 = 26.6$ g/particle

5.1.2 Side-shot Attack. Since the side-shot attack is going to be a thin plate hypervelocity collision, the first parameter that must be calculated before the mass of debris created can be predicted, is the size of the hole which will be left in the target by the projectile. In Section 4.2.1, Equation 23 calculates the ratio of the diameter of the hole made in a thin plate target (D) to the diameter of the projectile (d).

$$D/d = 0.45 \times 10 \times (0.74/0.196)^{2/3} + 0.90 = 11.8 \tag{54}$$

Since the diameter of the projectile is 0.196 meters, the diameter of the hole left in a thin plate target will be 2.31 meters (0.196 × 11.8). However, the side of the notional target is a cylinder and not a flat plate. Since the size of the hole, made in a thin-plate target, increases as the thickness of the target, it seems reasonable to infer the more target mass there is resisting projectile penetration, the larger the hole in the target. It should be recalled here that in a thin plate collision the projectile passes through the target. Since the target is not a true flat plate, the amount of target material the projectile "sees" will be less (see Figure 21). Thus, it seems the hole made in the notional target should be slightly smaller than one made in a true flat plate.

The ratio of the volume of a cylinder with (diameter of 2 and a rounded top and bottom with an arc of radius of one) to the volume of a cylinder with flat tops (diameter of 2) is 5.333/6.283 or 0.849.

$$\text{Vol} = 2 \int_{-1}^{1} \int_{-\sqrt{1-x^2}}^{\sqrt{1-x^2}} \sqrt{1 - y^2} \, dy \, dx = 5.333 \tag{55}$$

Reducing the value for the thickness of the target will make a better estimation for the size of the hole created in the target. The new adjusted value for the targets thickness will be 0.63 meters (0.849 × 0.74). Plugging this new value into the thin-plate hole-size equation gives

$$D/d = 0.45 \times 10 \times (0.63/0.196)^{2/3} + 0.90 = 10.7. \tag{56}$$
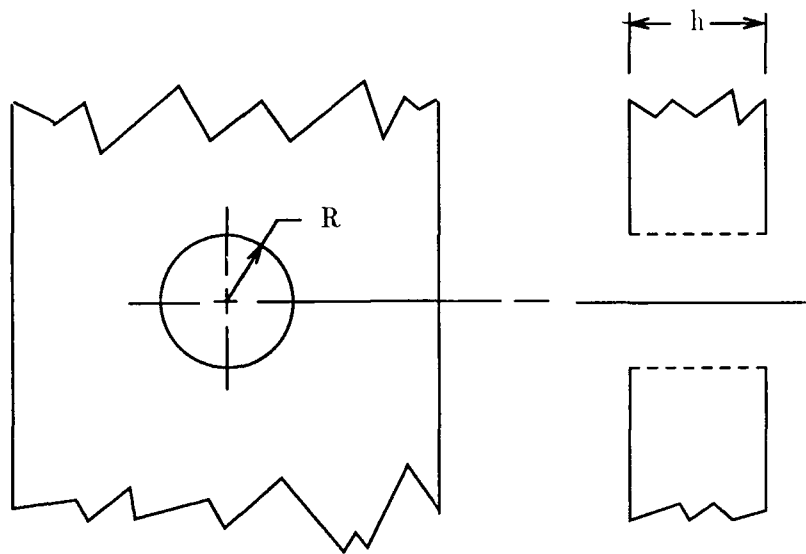
Hole in Flat Plate
Vol $= \pi R^2 h$
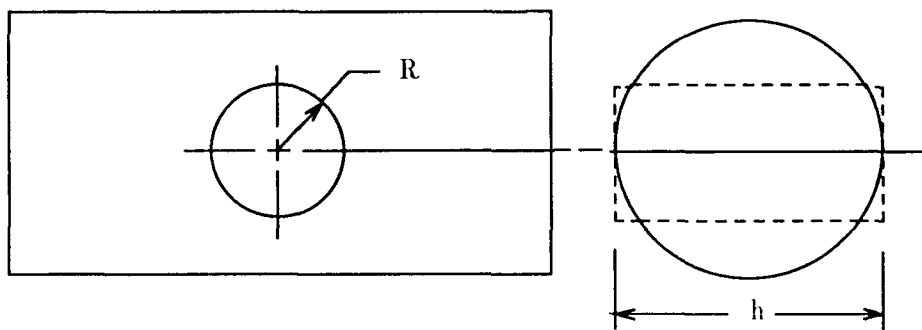
Hole in Cylinder

Vol $< \pi R^2 h$

Figure 21. Hole Volume Comparision
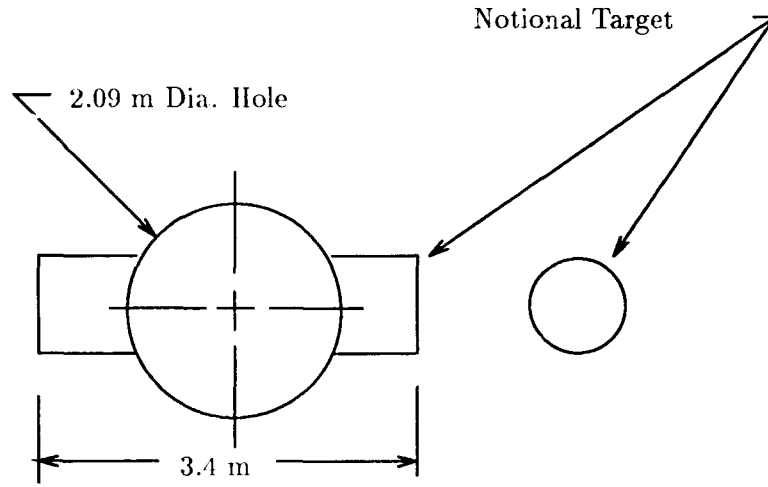
Figure 22. Hole in Notional Target from a Side-shot Engagement

The adjusted value for the diameter of the hole made in the side-shot engagement will be 2.09 meters (10.7 × 0.196). This hole is larger than the diameter of the target, so the projectile will probably cut the notional target in half, liquifying about 2 meters of the middle, and leaving about 0.7 meters on each side of the hole intact (see Figure 22).

A first approximation for the volume of target destroyed can be made using 2.16 as the height of the cylinder of target destroyed and 0.74/2 as the radius:

$$\text{Vol} = \pi \times (0.74/2)^2 \times 2.09 = 0.90 \, \text{cu. meters} \tag{57}$$

Integrating gives a more accurate estimation of the volume because the ends of the cylinder of target destroyed are curved, not straight:

$$\text{Vol} = 2 \int_{-0.37}^{0.37} \int_{-\sqrt{0.37-x^2}}^{\sqrt{0.37-x^2}} \sqrt{1.092 - y^2} \, dy \, dx = 0.885 \, \text{cu. meters} \tag{58}$$

Multiplying the volume by the target will give the mass of debris produced:

$$M_c = 0.885 \times 2,710 = 2,400 \, \text{kg} \tag{59}$$

62

Plugging in the above values gives

$$N = 0.8(.00141/2,400)^{-0.8} = 77,200. \tag{60}$$

So, in the side-shot engagement, 2,400 kg of debris will be produced in 77,200 pieces with diameters greater than 1 cm. This is about twice the mass of debris produced by the same projectile against the same target as in the end-on engagement. This is consistent with the results obtained in debris production in thin plate collisions because a given projectile has the potential to generate more debris colliding with a thin-plate target than in any other type of collision.

To a lesser degree, target strength and target temperature also play a role in determining the amount of debris produced by a given projectile. More debris will be produced by a projectile colliding with a warmer and weaker target, if all other factors remain the same. However, there is not good agreement in the literature on just how much target strength and target temperature affect debris production. The data that is available suggests they are an order of magnitude less significant, in determining debris production, then the mass and velocity of the projectile.

For a very precise estimation of debris dispostion, target strength and temperature will need to be considered; however, the level of accuracy possible in this methodology is not great enough to allow for such precision. Thus, temperature and strength effects will be ignored.

5.2 SOLWIND ENGAGEMENT

Since the United States has actually destroyed a satellite in orbit, it would seem a reasonable exercise to use hypervelocity impact theory to predict what actually happened when the Miniature Homing Vehicle, launched from the F-15, impacted with the Solwind solar observing satellite. This prediction will differ from the notional satellite engagement example in one major way. There is data available to check the validity of the prediction. The Space Surveillance Center tracked and catalogued the debris which resulted from the break-up of solwind. By plotting the debris orbits backward in time, to the time of impact, it is hoped the nature of the impact can be verified.

5.2.1 The Prediction. In predicting what happened to Solwind, first the mass ratio of the projectile to the target will be calculated. The projectile has a mass of 16 kg and the target 878 kg. The ratio is then $878/16 = 54.9$. This is well below the 115 cutoff specified by Kessler as the limit for a catastrophic collision. Thus, if the projectile hit the most massive part of Solwind, a catastrophic collision should have occurred.

But, looking at Figure 28 shows a large area of Solwind is composed of solar panels. Since the area of the solar panels is about two-thirds the area of the satellite (as seen from the side), it is likely the projectile collided with the solar panels. If this is the case, the solar panels were probably shattered and the base of the satellite left intact. According to the Air University's *Space Handbook*, solar panels weigh about 1 pound per square foot. The area of the solar panels is close to 47 square feet. Thus, if only the solar panels were hit by the projectile, 47 lbs or 21.3 kg of debris were produced and the 16 kg projectile, as well as the 850 kg base of the satellite, were left largely intact.

The other alternative is the projectile hit the main body of the satellite, and a catastrophic collision resulted. In this case, all of Solwind and the entire projectile were converted to debris. This comes to a total of 894 kg $(878 + 16)$ of debris.

5.2.2 *Verification.* In attempt to verify what actually did happen to Solwind, Major T.S. Kelso obtained several sets of orbital elements from the Solwind debris. He took the data and selected the sets that were most consistent in arriving backward to the correct time of impact. From these selected element sets, he plotted 18 pieces of debris on two, three dimensional computer displays showing a view of the earth from space (see Figures 23 and 24). The arrow indicates the location of the collision between the Miniature Homing Vehicle and Solwind. It is rewarding the location of the collision is near the west-coast of the United States, as the F-15 which launched the Miniature Homing Vehicle took off from Edwards Air Force Base, California. In these displays, a snapshot of the debris location is taken every four minutes . As the figures illustrate. he debris comes apart from the point of impact and then travels in approximately the same orbit as Solwind before the impact. This is consistent with figures in the orbital debris literature which depict debris from explosions in orbit describing donut shaped volumes of space around the original orbit. However, the fidelity of this view could not show the vectors of the individual debris fragments, but it could help eliminate two possible collision types. If there had been a thick target type of collision, all of the debris produced should have left the impact area ahead of Solwind's position had there been no collision (see Figure 17). This is not what occurred. Some of the debris went ahead of Solwind, but about two-thirds of the debris left the impact site behind Solwind. So it can be said, fairly confidently, that a thick target collision did not occur.

In a thin plate collision, about two-thirds of the debris will exit the rear of the target. In this type of collision, little debris is propelled perpendicular to the projectile's trajectory. Referring to Figures 25, 26, and 27, a large portion of the debris in the Solwind engagement did exit the impact site at right angles to the projectile tragectory (The X-axis is the direction Solwind was traveling before the impact, the Y-axis is toward the center of the earth, and the Z-axis is the Angular Momentum vector.) From these three views of the debris velocity vectors. it appears unlikely a thin plate collision occured.

This leaves a catastrophic collision. Is there a way to determine if the entire satellite was destroyed, or only the solar panels? In an attempt to answer this question, the radar cross section of all 250 catalogued pieces of Solwind debris were added together. The total was 42.8 square meters. This is roughly six times the original radar cross section of Solwind (7.04 sq. m). This, along with the fact that 5 largest of the 250 pieces of debris alone account for more radar cross section than the solar panels originally did, leads to the conclusion that the Miniature Homing Vehicle collided with the main body of Solwind and a catastrophic collision resulted, which destroyed the entire satellite.
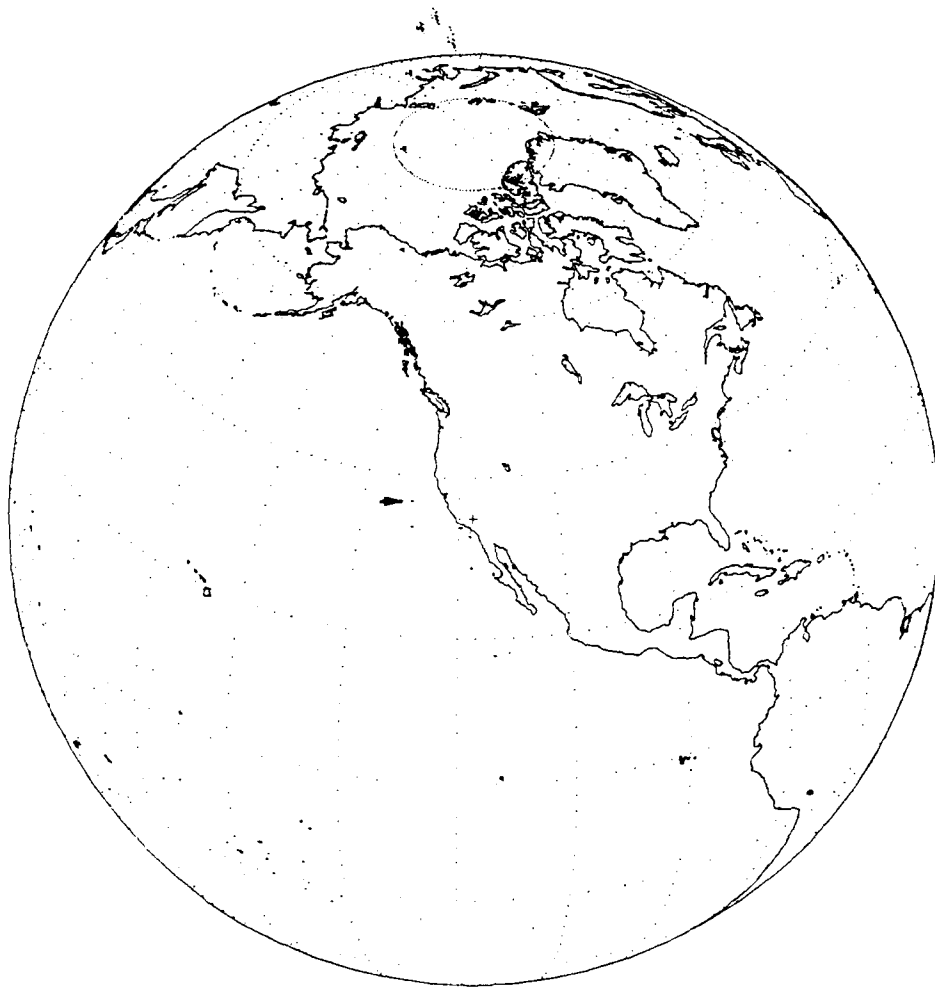
Figure 23. Overhead View of Solwind Engagement
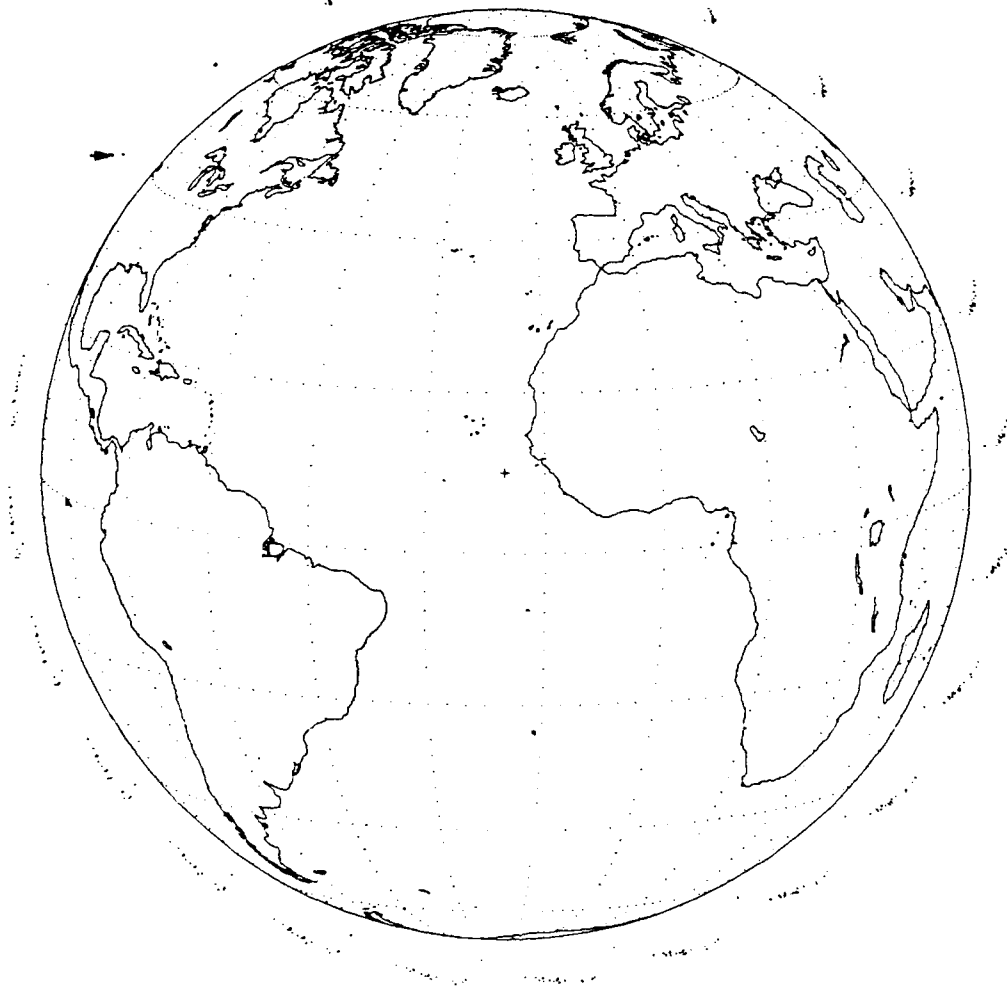
Figure 24. Side View of Solwind Engagement

13 Sep 85, 204243 UTC

— 10 m/s
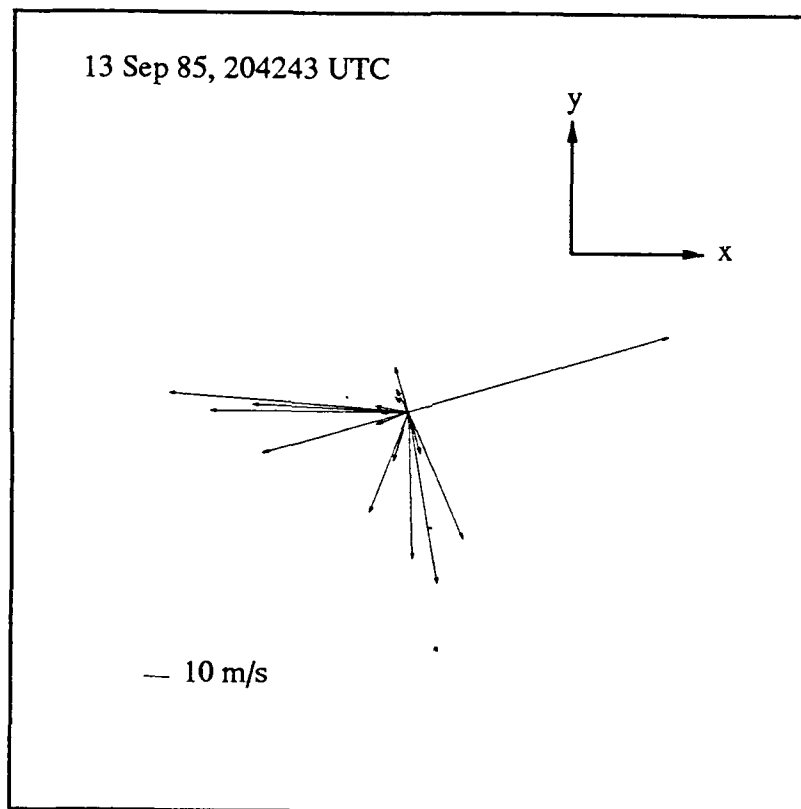
Figure 25. Velocity of Solwind Debris Particles Shortly After Impact (X-Y Plane)

69
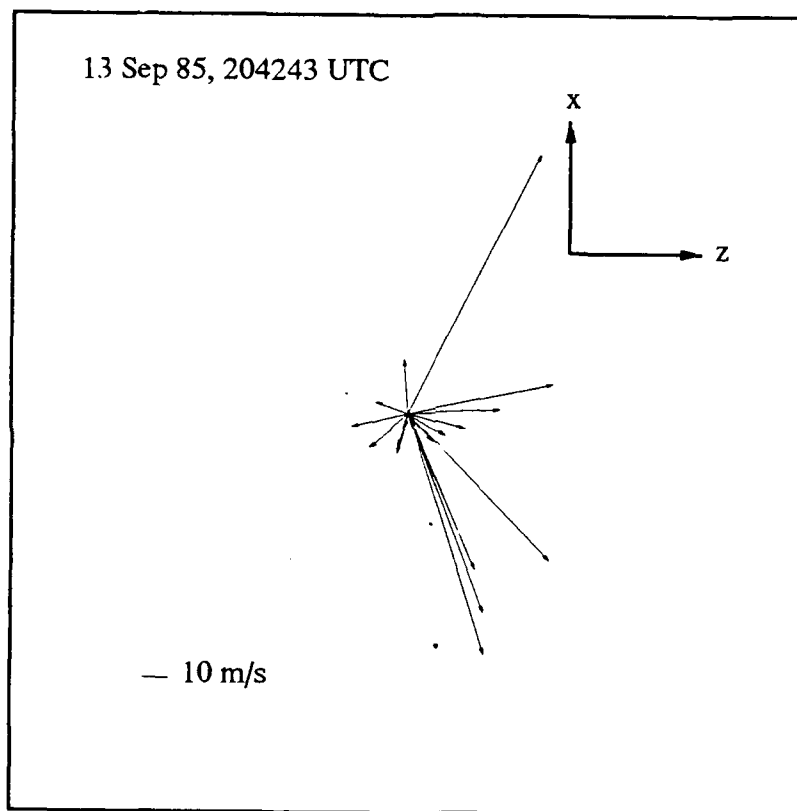
Figure 26. Velocity of Solwind Debris Particles Shortly After Impact (X-Z Plane)
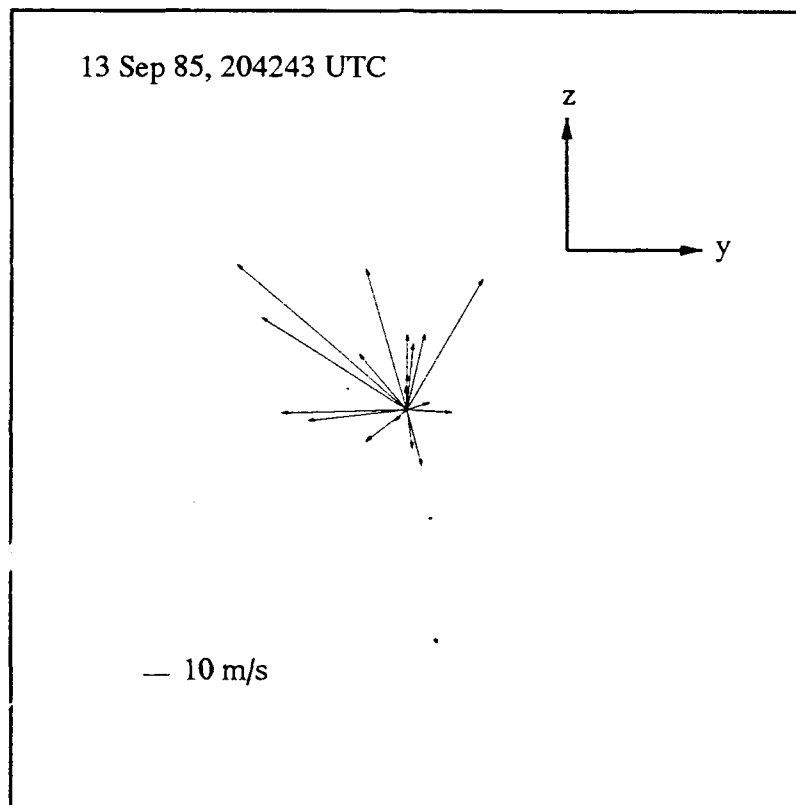
Figure 27. Velocity of Solwind Debris Particles Shortly After Impact (Y-Z Plane)

VI. Conclusions and Recommendations

6.1 CONCLUSIONS

For a commander to minimize debris production in ASAT engagements, he must consider the closing velocity of the projectile with the target, the target-projectile mass ratio, the density of the target and projectile, and the attack orientation. In general, he will want to hit the thickest part of the target with the smallest projectile that will incur the amount of damage required to kill the satellite. As projectile-target closing velocity is increased, the mass of the projectile required to obtain a kill is reduced. Reducing projectile size will reduce the amount of debris produced and also reduce the likelihood the engagement will result in a catastrophic collision.

This study suggests a large amount of debris will be produced when a kinetic energy weapon, traveling at hypervelocity, collides with a satellite in orbit. Although using a direct-ascent kinetic energy weapon is probably the least expensive means to accomplish the ASAT mission, there are costs to the space environment which mitigate the utility of this type of weapon. In a hypervelocity impact between a kinetic energy projectile and an average size satellite, thousands of new satellites are created, posing a hazard to manned and unmanned spacecraft for years or perhaps centuries after the ASAT engagement. At the very least, it is likely the residual debris, from the engagment, will make the target satellite's original orbit unusable for several years. It seems that space is an environment sufficiently challenging without the addition of man-made hazards.

6.2 RECOMMENDATIONS

1. Don't use kinetic energy projectiles against targets in space.

2. Explore alternate, non-destructive, ways to negate satellites. This could include devising a means to enshroud a target satellite with a reflective mylar-like cover. If the satellite cannot receive commands from the ground and cannot transmit its data, it is as good as dead and no debris is generated (except that generated getting the "satellite bag" into space).

   Another possible method to negate satellites without creating orbiting debris is to develop a co-orbital hunter-killer which could rendezvous with the target satellite, connect to it somehow (possibly with some type of robot arm), and then fire a breaking motor. A sufficient impulse by the braking motor would cause the satellite to reenter the atmosphere. If such a large magnitude of thrust is impractical (expensive), less of an impulse could alter the target satellite's orbit. A significant change in the ellipticity or the period of the target satellite's orbit would probably make it unable to execute its mission.

3. If it is decided the tactical benefits of using a kinetic energy weapon to attack a satellite outweigh the attendant risks to future space operations, measures should be taken to minimize the amount of debris produced during the attack.

   First, as satellites exist today, they are not robust systems. If, say, as little as ten percent of a satellite mass is destroyed in an attack, it is likely it will no longer function. Weight is critical when designing space systems, therefore they are not armored to any significant degree and there is very little onboard a satellite that is not essential for it to carry out its mission. Almost everything onboard is needed for day-to-day operations. Taking out a satellite's amplifier, receiving or transmitting antenna, receiver, or payload subsystems will "kill" the satellite. If it can't get its data to the ground, it is as good as dead. Even if some vital subsystem isn't physically destroyed in the ASAT engagement, the shock wave created by a collision with a kinetic energy projectile will probably scramble one or more of its vital electrical components, leaving the satellite a useless astronomical oddity.

With this in mind, it is not necessary for an ASAT weapon to obliterate the target spacecraft for its mission to be successful. In fact, for debris minimization purposes, the opposite approach must be taken. What is the least amount of damage that must be inflicted to render the satellite dead? Upon consultation with others with operational experience with satellites, a figure of 10 percent was obtained which will be used as the mass of the satellite that must be destroyed for to obtain a 95 percent probability of a kill (PK). Of course this figure is somewhat arbitrary. It could be higher *or it could be significantly lower.* But until reliable figures are generated, it will have to serve.

It is assumed that ASAT weapons will be directed against specific target satellites. Commanders will want to destroy intelligence gathering platforms, command and control satellites, and perhaps global navigation satellites. A specific ASAT mission will be launched against a specific target. Thus, the mass and density of the target will be known and the amount of mass that must be destroyed can be calculated.

To minimize debris production, a commander should use the smallest kinetic energy weapon available that will destroy the required 10 percent of the satellite. This will first minimize the mass of booster and attendant debris required to get the projectile into orbit as a smaller projectile requires a smaller booster to achieve the same orbit. This will also reduce debris generated by the projectile itself. To achieve this, several sizes of kinetic energy weapons will have to be available, since satellites vary in size.

To determine what size projectile must be used, the mass of the target (M_2) must be known. Then multiply this figure by 10 percent. For a 4,000 kg RORSAT, 400 kg of satellite must be destroyed to obtain our PK of 95 percent. From laboratory experiments conducted by E.P. Palmer and G. H. Turner (21:18), in which they make energy measurements using 3/16-inch diameter chrome-steel balls fired into lead targets, it was determine that 114 joules yields one gram of debris (or 114,000 Joules/kg). If it is assumed that it takes about the same magnitude of energy to create debris from a satellite materials, the amount of energy required to destroy 400 kg of satellite can be calculated.

$$E_{req} = 114,000 \times 400\,\text{kg} = 45.6\,\text{Mjoules} \tag{61}$$

Of course, in a kinetic energy weapon, all of the energy that it can impart upon the target is in the form of kinetic energy. Solving $E_k = 1/2MV^2$ for M yields:

$$M_1 = \frac{2\,E_k}{V_p^2} = \frac{2(114,000\frac{M_2}{10})}{V_p^2} = \frac{22,800 M_2}{V_p^2}. \tag{62}$$

The only unknown is the velocity of the projectile relative to the target. From the above equation, it can be seen that to minimize the mass of the projectile required, the velocity of the projectile must be maximized. To do this, the projectile should be launched into the same orbit as the target, but *traveling in the opposite direction*. This will result in closing velocity of about 15 km/s. Substituting this value into the above equation gives: $(2(45.6 \times 10^6))/15,000^2$ which equals **0.41 kg**.

So, 1/2 kilogram projectile can theoretically kill a RORSAT, if it is placed in the correct orbit. This figure also assumes the projectile is stopped by the target and does not merely perforate a thin structure onboard the satellite, such as an antenna or solar panel. To be most effective the projectile must impact the most massive part of the target satellite.

# Appendix A. *The U.S. F-15 Launched ASAT Program*

A.1 *The Third Test*

An F-15 fighter raced off a runway at California's Edwards Air Force Base last Friday (13 Sept, 1985), soared to 35,000 ft., then launched an 18-ft.-long, two-stage rocket. At the same time, some 320 miles above the Pacific, an inoperative six-year-old satellite hurtled along at 17,000 m.p.h. A 35-lb. instrument package, no larger than a gallon can, separate from the rocket. Guided by infrared sensors that could detect the warmth of the satellite and powered by 64 tiny jet rockets, the cylinder closed in on its target. *Zap!* The two bodies collided at a combined speed of almost 27,000 m.p.h. The satellite was destroyed. (27:29)

This month's successful test of the ASAT system, the third in a planned series of 12 and the first against a satellite in space, was achieved after a delay of several months while weapon and target system difficulties were resolved (AW&ST Sept. 2, p. 20).

The Sept. 13 launch of the ASAT, consisting of a Boeing short-range attack missile (SRAM) first stage, an LTV Altair second stage and an LTV-developed miniature homing vehicle warhead, was the first test firing of the system since last November (AW&ST Nov. 19, 1984). Although the latest ASAT was originally scheduled to be fired against an instrumented target vehicle launched by an LTV Scout rocket, problems with communications gear on board the target vehicle ultimately resulted in a decision to fire the weapons against a live satellite in space. The target of the test firing this month was an Air Force Space Test Program satellite called P78-1, known also by the name of is primary experimental payload, the Defense Advanced Projects Research Agency gamma ray spectrometer. The satellite also had six secondary experimental payloads, including three from the Navy, two from the Air Force and one from the Army.

The 1,936-lb., 11.3-ft.-long, 6.8-ft.-dia. satellite was built by Ball Aerospace Corp. and launched in February, 1979, into a circular polar orbit inclined 97.7 deg. at 320 naut. mi. It had a planned mission duration of 12 months. Although U.S. Air Force officials said the satellite had outlived its useful life, it was still transmitting data to Earth up to the moment it was struck and disable by the ASAT...Air Force officials said telemetry signals from both the satellite and the ASAT miniature homing vehicle stopped at exactly the same time, indicating that the ASAT had in fact struck the satellite.

Hitting the actual satellite was considered slightly more difficult than hitting the instrumented target vehicle originally scheduled to be used in the test, according to Air Force officials. (26:20-21)
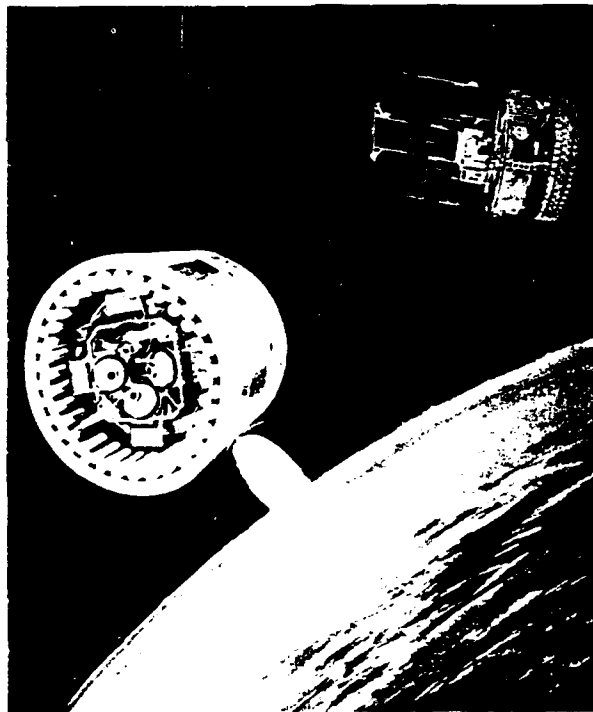
An F 15 releases its ASAT payload 13 September 1985 (top) to destroy the still active Solwind solar-observing satellite (bottom). The trial was highly successful but Congress refused to permit further tests and USAF cancelled the programme in March 1988. *(LTV)*

Figure 28. U.S. ASAT Program

A.2 The Second Test

Los Angeles—Air Force tested the miniature homing vehicle payload on its anti-satellite missile for the first time Nov. 13 (1984) when the 17-ft.-long missile was launched from a USAF/McDonnel-Douglas F-15 aircraft in airspace over the Western Test Range...Primary objective of last week's test was to demonstrate the capability of the miniature vehicle flight sensor to acquire and track a fixed infrared-emitting object. The miniature vehicle has a flight sensor that acquired and tracks a target, with a computer using flight sensor information to calculate and command the necessary maneuvers for intercept and a propulsion system.

The missile separated from the F-15, flew to a predetermined position in space, acquired a target—which for this test was a star—and deployed the miniature vehicle, with the flight sensor continuing to track the star through a portion of the miniature vehicle's trajectory.

The missile was launched from one of two F-15's modified to carry ASAT missiles. Air Force officials said none of the components of the antisatellite system went into orbit, and that all parts of the system landed in the Pacific Ocean within the Western Test Range. (25:20-21)

A.3 The First Test

On 21 January, 1984 the U.S. Air Force conducted the first flight test of its new ASAT missile.

The ASAT missile, which carried a simulated miniature (homing) vehicle, was launched by the F-15 toward a point in space, although no part of the weapon system went into orbit. No target was involved in the test.

Purpose of the test of the two-stage booster and guidance system was to determine the effects of launching the missile from the aircraft, as well as booster and guidance performance...The initial flight test follows about one year of aircraft compatibility testing at Edwards AFB, Calif., including 15 captive carry tests of the 17-ft.-long missile. The F-15 has a special pylon for carrying the 2,700 lb weapon and a pallet in the aircraft's ammunition bay.

Flight tests are designed to evaluate overall system performance, including aerodynamics, propulsion, accuracy and navigation and guidance. (24:19)

A.4 Prologue

The US military have felt the need for a system capable to destroying po-
tentially hostile orbiting satellites since the beginning of the space era. The
first test of such a system was Bold Orion. An air-launched missile scored a
deliberate near-miss on the US Explorer 6. That was followed by SAINT, var-
iously reported to be acronym for SAtellite INspector, SATellite INTerceptor,
or SAtellite Inspection and NegaTion. That was cancelled in 1962 without
any flight tests, and was followed by an ASAT system that would have used
nuclear-tipped Thor missiles based on Johnston Island in the Pacific. Tests
were flown, apparently without nuclear warheads, and President Johnson de-
clared the system operational in 1964. It was dismantled in 1975, although by
then Soviet ASAT tests had been under way for 7 yr.

Development of the more recent USAF ASAT system began under President
Ford following concern that the Soviet system was by then operational. (32:259)

A.5 Epilogue

A.5.1 The Death of the ASAT Program

The Congressional ban imposed in year-long blocks since September 1985
against anti-satellite (ASAT) testing on objects in space automatically ended 30
September 1987, with the USAF hoping to launch threee intercept demonstra-
tions during 1988, awarding a $78 million contract to LTV's Missiles Division
in late September for continued ASAT work....The Congressional ban was ex-
tended, however, and all the launches were deleted by the time March 1988's
ELV listing was released. The USAF's initial projection of a fully operational
system by 1989, and then by the early 1990s, was untenable and the project's
cancellation was announced. (32:258)

A.5.2 Rebirth

(23 July, 1990) Rockwell International Corp. is the sole winner of a U.S.
Army competition to design a $2-billion antisatellite weapon.

The Pentagon had planned to select two contractors for the ASAT demon-
strration and validation effort, which is projected to last two years and be worth
about $100 million to the El Segundo, Calif., company.

The Army expects to award the contract in about 30 days.

McDonnell Douglas and Lockheed submitted proposals as well. But with
spending on all sorts of Pentagon programs being slashed, the Defense Dept.
opted to save money on ASAT.

"There wasn't a great deal of difference in the technical approach of the three proposals," William M. Congo, the U.S. Army Strategic Defense Command's chief of external affairs, said. "This is the time to be prudent and save."

The Army leads the armed forces' effort to create a single-site, ground-based, "transportable," kinetic-kill missile system capable of destroying satellites in orbits up to 2,000 km (1,080 naut. mi.).

According to senior Defense officials, such an antisatellite weapon would give the U.S. an advantage in a conventional war and could be built and operated for 20 years for $2-2.5 billion. Contrary to longstanding assumptions, even if the U.S. were to suffer the loss of similar spacecraft in retaliation, destroying Soviet satellites in low Earth orbit offers an advantage in theater warfare, the Pentagon has determined. (2:30)

Appendix B. *The Soviet Ocean Reconnaissance Satellite Program*

For the past 29 years the Soviets have conducted a spaceborne monitoring program designed to detect, locate and classify potentially hostile naval surface vessels. Such information would be extremely useful during a conflict, allowing precise targeting of hostile naval surface groups for anti-ship missile launched from Soviet air, surface or subsurface platforms. The magnitude of the threat caused by these satellites to US carrier battle groups was demonstrated when the US Department of Defense cited Soviet ocean reconnaissance spacecraft as one of the primary justification for the development of an American anti-satellite capability.

Two types of satellites compose the space-based component of the Soviet ocean surveillance program. The radar ocean reconnaissance satellite system (dubbed RORSAT by US defense analysts) is designed to located large surface vessels and concentrations of smaller ships via active illumination by radar energy. The ELINT ocean reconnaissance satellite system (or EORSAT) locates hostile fleet elements by collecting the emissions of their radar and communications systems. This section describes the physical and operational characteristics of these tow spacecraft and provides a tabular launch history of their missions.

The first vehicle test for RORSAT was conducted in 1967. The spacecraft is always launched from Tyuratam on an F-1m (SL-11) booster. RORSAT operational parameters generally include almost circular orbits with perigees between 250 and 260 kilometers, inclined at 65 degrees, with orbital periods of 89.5 minutes. The spacecraft is composed of the vehicle itself and a non-separating third stage of the booster. An ion engine is attached to the spent booster stage for orbital maintenance (the choice of a mean 255-kilometer altitude represents a trade-off between the power of RORSAT's sensor and the probability of detecting objects on the ocean's surface). Forward of the F-1m (SL-11) launch vehicle's third stage is an instrument module that carries the RORSAT's electronic and attitude control instrumentation. Communications equipment in the instrument module broadcasts at 19 Mhz. Beyond the instrument module is the radar antenna, which has been described in open Western sources as either a planner array or a slot-type antenna. The antenna is attached to the main body of the vehicle, which contains a boost stage for placing the power supply module in a higher orbit at the end of mission life. Two antennas protrude from the forward section of the main body, which contains a boost-stage electronics module that transmits at 19.542 Mhz. The power supply is mounted on the nose of the spacecraft. It is a Topaz thermionic reactor-convertor which supplies 10 kW of power.

RORSAT has been one of the most error-plagued elements of the Soviet space program. The majority of difficulties stems from its reliance upon nuclear power and the resulting danger of contamination, should a RORSAT deorbit in such a way as to allow the reactor core to survive reentry. From the beginning of the program, Soviet mission planners have sought to prevent just such an occurrence by boosting the reactor to a 900 to 1,000 kilometer orbit, from which it will not decay for hundreds of years. (The other components of the vehicle remain in low-earth orbit, from which they decay naturally in a few days or weeks.) The 16th RORSAT (Kosmos 954), however, failed to execute the lofting maneuver for its reactor at the end of its mission life. In early November 1977 the spacecraft entered a decaying orbit, and, following the loss of attitude control in early 1978, deorbited over northern Canada. Radioactive debris was scattered over a large area of the essentially unpopulated Canadian tundra. A joint US-Canadian clean-up effort decontaminated most of the effected area, and the Soviet RORSAT program entered a two-year hiatus.

Kosmos 1176, the next RORSAT launch, demonstrated the solution chosen by the Soviets to meet the problem of premature reentry of the reactor module. Reasoning that the reactor housing had shielded the radioactive fuel core from the effects of reentry, Soviet specialists redesigned the vehicle's boost stage to permit the ejection of the core so as to maximize the chances that radioactive debris would not reach the surface of the planet. The next six RORSATs following Kosmos 1176 performed the tripartite separation and the reactor lofting maneuver, followed by the ejection of the core once the reactor had reached an altitude of roughly 900 kilometers.

The Soviets had the chance test their modified nuclear safety procedures when, in late 1982, Kosmos 1402 encountered end-of-mission difficulties. Vehicle separation yielded only two segments rather than the intended three, and when it apparently became impossible to boost the reactor to a higher orbit, Soviet mission controllers ejected the core. The reactor deorbited over the Indian Ocean on 24 January 1983. Two weeks later, the reactor core reentered the atmosphere over the south Atlantic.

Very little of the radioactive debris from Kosmos 1402 apparently reached the planet's surface, but the Soviets could not have been pleased by the second mission failure in five years. Another hiatus in RORSAT launches followed, this time lasting a year. Evidently the Soviets decided to add further modification to the vehicle, the mission control apparatus or both. These changes have not been apparent since the resumption of RORSAT flights in 1984, and may not be until another lofting failure occurs.

In a larger sense, even successful boostings of reactors into (higher) orbit may be dubious achievements. Western specialists have pointed out that the debris from Kosmos 942 contained radioactive isotopes of Uranium-235 (93 percent enriched). While the parking orbits for the reactor housings and cores assure reentry in 300 to 1000 years, the half-life of U-235 is over 70,000 years. When the lofted RORSAT elements eventually do reenter, they will still pose a major threat of contamination, especially those elements in the 15 reactors boosted before Kosmos 954, which have not ejected their cores.

...Resolution of RORSAT has been reported in the Western press to be destroyer-sized objects in calm seas and carrier-sized objects (or clusters of smaller vessels) in rough seas...Targeting data derived from Soviet ocean reconnaissance satellites can be down-linked in real-time to platforms capable of receiving such transmissions. They can also be passed in a less timely manner through ground reception sites in the USSR to deployed forces without means of direct reception.(10:43-44)

Table 4 provides the history of RORSAT launches.

No.	Name	Satellite Number	Launch Date	Termination Date	Lifetime
1	Kosmos 198	3081	27 DEC 67	28 DEC 67	1 day
2	Kosmos 209	3158	22 MAR 68	23 MAR 68	1 day
3	Kosmos 367	4564	3 OCT 70	3 OCT 70	< 3 hours
4	Kosmos 402	5105	1 APR 71	1 APR 71	< 3 hours
5	Kosmos 469	5721	25 DEC 71	3 JAN 72	9 days
6	Kosmos 516	6154	21 AUG 72	22 SEP 72	32 days
7	Kosmos 626	7005	27 DEC 73	9 FEB 74	45 days
8	Kosmos 651	7291	15 MAY 74	25 JUL 74	71 days
9	Kosmos 654	7297	17 MAY 74	30 JUL 74	74 days
10	Kosmos 723	7718	2 APR 75	15 MAY 75	43 days
11	Kosmos 724	7727	7 APR 75	11 JUN 75	65 days
12	Kosmos 785	8473	12 DEC 75	12 DEC 75	< 3 hours
13	Kosmos 860	9486	17 OCT 76	10 NOV 76	24 days
14	Kosmos 861	9494	21 OCT 76	20 DEC 76	60 days
15	Kosmos 952	10358	16 SEP 77	7 OCT 77	21 days
16	Kosmos 954	10361	18 SEP 77	31 OCT 77	43 days
17	Kosmos 1176	11788	29 APR 80	10 SEP 80	134 days
18	Kosmos 1249	12319	5 MAR 81	18 JUN 81	105 days
19	Kosmos 1266	12409	21 APR 81	28 APR 81	8 days
20	Kosmos 1299	12783	24 AUG 81	5 SEP 81	12 days
21	Kosmos 1365	13175	14 MAY 82	26 SEP 82	135 days
22	Kosmos 1372	13243	1 JUN 82	10 AUG 82	70 days
23	Kosmos 1402	13441	30 AUG 82	28 DEC 82	120 days
24	Kosmos 1412	13600	2 OCT 82	10 NOV 82	39 days
25	Kosmos 1579	15085	29 JUN 84	26 SEP 84	90 days
26	Kosmos 1607	15378	31 OCT 84	1 FEB 85	93 days
27	Kosmos 1670	15930	1 AUG 85	22 OCT 85	83 days
28	Kosmos 1677	15986	23 AUG 85	23 OCT 85	60 days
29	Kosmos 1736	16647	21 MAR 86	21 JUN 86	92 days
30	Kosmos 1771	16917	20 AUG 86	15 OCT 86	56 days
31	Kosmos 1860	18122	18 JUN 87	28 JUL 87	40 days
32	Kosmos 1900	18665	12 DEC 87	14 APR 87	124 days
33	Kosmos 1932	18957	14 MAR 88	19 MAY 88	66 days

Table 4. Soviet Orbital RORSAT Program History
(14:74)

Bibliography

1. Air University *Space Handbook*. Maxwell AFB, AL, Air University Press, January 1985.

2. Asker, James R. "Rockwell Selected as Sole Contractor For $100-Million Asat Design Effort," *Aviation Week & Space Technology*, 133:30, 23 July, 1990.

3. Bennett, Gary L. "A Look at the Soviet Space Nuclear Power Program," *International Forum on Energy Engineering*, Washington D.C., NASA, August 1989.

4. Bess, T. D. *Mass Distribution of Orbiting Man- Made Space Debris*, "NASA Technical Note TND-8108, 1975," Washington D.C., 1975.

5. Cintala, M. J. et al., "The Nature and Effects of Impact Cratering on Small Bodies," *Asteroids*, (A80-24551 08-91) Tucson, AZ, University of Arizona Press, 22:579-600, 1979.

6. Chou, Pei C. et al., *Dynamic Response of Materials to Intense Impulsive Loading*, Wright-Patterson AFB, OH, Air Force Materials Lab, 1972.

7. Diedrich, I.J. and F. S. Loeffler, "Brittle Behavior of Beryllium, Graphite, and Lucite Under Hypervelocity Impact," *Proceedings of the 7th Hypervelocity Impact Symposium*, Vol. 6, 27-47, U.S. Army, Navy, Air Force, 1965.

8. Department of Defense *Soviet Military Power 1985*. Washington D.C., U.S. Government Printing Office, April 1985.

9. Fish, Richard H. and James L. Summers, "The Effect of Material Properties on Threshold Penetration," *Proceedings of the 7th Hypervelocity Impact Symposium*, Vol. 6, 1-26, U.S. Army, Navy, Air Force, 1965.

10. Hart, Douglas. *The Encyclopedia of Soviet Spacecraft*. New York, Bison Books Corp., 1987.

11. Henderson, B. J. and A. R. Zimmerschied. *Very High Velocity Penetration Model*. Boeing Aerospace Co., Physics Dept., Seattle, WA, May 1983.

12. Henderson, Breck. "Sandia Researchers Test 'Coil Gun' For Use in Orbiting Small Payloads," *Aviation Week & Space Technology*, 132, No. 19, 2: 88-89, May 7, 1990.

13. Johnson, N.L. "Orbital Phasings of Soviet Ocean Surveillance Satellites." *Journal of Spacecraft and Rockets*. March-April 1982.

14. Johnson, Nicholas L. *The Soviet Year in Space, 1988*. Colorado Springs, CO, Teledyne Brown Engineering, 1989.

15. Kessler, Donald J. and Burton G. Cour-Palais. "Collision Frequency of Artificial Satellites: The Creation of a Debris Belt," *Journal of Geophysical Research*, 83, A6, 10: 2637-2646, 1 June 1978.

16. Kinslow, Ray (editor). *High-Velocity Impact Phenomena*. New York and London, Academic Press, 1970.

17. Maiden, C.J. et al., "Thin Sheet Impact," *Proceedings of the 7th Hypervelocity Impact Symposium*, Vol. 4, 63-123, U.S. Army, Navy, Air Force, 1965.

1ᴜ. Miller, Franklin Jr. *College Physics* (4th Ed.), New York, Harcourt Brace Jovanovich, Inc., 1977.

19. Moore, H. J. et al. "Change of Effective Target Strength With Increasing Size of Hypervelocity Impact Craters," *Proceedings of the 7th Hypervelocity Impact Symposium*, Vol. 4, 35-46, U.S. Army, Navy, Air Force, 1965.

20. Naumann, Robert J. "A Physical Basis for Scaling Hypervelocity Impacts," *Proceedings of the 7th Hypervelocity Impact Symposium*, Vol. 4, 35-46, U.S. Army, Navy, Air Force, 1965.

21. Palmer, E.P. and G. H. Turner "Energy Partitioning in High-Velocity-Impact Cratering in Lead," *Proceedings of the 7th Hypervelocity Impact Symposium*, Vol. 5, 35-46, U.S. Army, Navy, Air Force, 1965.

22. Riney, T.D. and J. F. Heyda, "Hypervelocity Impact Calculations," *Proceedings of the 7th Hypervelocity Impact Symposium*, Vol. 2, 77-185, U.S. Army, Navy, Air Force, 1965.

23. Roark, Glenn L. *Hypervelocity Impact of Active Pellets*. Air Force Armament Laboratory, Air Force Systems Command, Eglins AFB, FL, 1967.

24. Staff. "USAF Tests Asat Weapon." *Aviation Week & Space Technology*, 120:19, 30 January, 1984.

25. Staff. "Air Force Tests Antisatellite Payload." *Aviation Week & Space Technology*, 121:28, 19 November, 1984.

26. Staff. "Defense Dept. Plans Next Test Firing of Air-Launched Asat System." *Aviation Week & Space Technology*, 123:20-21, 23 September 1985.

27. Staff. "Zap! Then a Flap." *Time*, 126:29, 23 September 1985.

28. Stares, Paul B. *The Militarization of Space*. Ithaca, New York, Cornell University Press, 1985.

29. Thomson, Robert G. and E. T. Kruszewski. "Effect of Target Material Yield Strength on Hypervelocity Perforation and Ballisitic Limit," *Proceedings of the 7th Hypervelocity Impact Symposium*, Vol. 5, 273-320, U.S. Army, Navy, Air Force, 1965.

30. Vitt, Elmar. "Space Debris," *Space Policy*, 5, No. 2, pg. 130, May 1989.

31. Wiesel, William E. *Spaceflight Dynamics*. New York, McGraw-Hill Book Company, 1989.

32. Wilson, Andrew (Editor). *Space Directory.* Geneve, Switzerland, Interavia SA, 1989.

33. Wilson, G.C. "Antisatellite Effort Needed, Senate Is Told," *Washington Post.* 24 April 1987.

34. Woolf, Henry B. et al. *Webster's New Collegiate Dictionary.* Springfield, Massachusetts: G. & C. Merriam Company, 1977.

35. Zukas, Jones A. et al., *Impact Dynamics*, New York, John Wiley & Sons, 1982.

Vita

Captain Stephen K. Remillard was born 8 February 1956 in Los Angeles, California. He graduated high school in Pinole, California in 1974. He attended U.C. Berkeley, De Anza College (received an A.A. degree), the University of Idaho and then spent three years as an infantryman in the U.S. Army. After leaving the Army, he attended San Jose State University where he received his bachelor's degree in Biological Science. From June 1984 until December 1985 he completed work at the University of Arizona towards a second undergraduate degree in Aerospace Engineering. In February 1986 he entered the Air Force and attended OTS and the Intelligence Officer training at Lowry AFB in Colorado. His first assignment was as a Current Intelligence Analyst/Briefer for the Foreign Technology Division (FTD), Wright-Patterson AFB, OH. Next, he was chosen to be the Chief of the FTD Special Security Liaison Office to the Aeronautical Systems Division (ASD), where he managed the SCI security program for over 2,000 active duty and government civilians at Wright-Patterson and contractors from all over the country. He next served as the Director of INS for the Foreign Technology Division where he managed the SCI security program for FTD. Then he entered the Space Operations program at the Air Force Institute of Technology in May, 1988.

Permanent address: 6048 Leycross Dr.
                   Huber Heights, Ohio 45424

REPORT DOCUMENTATION PAGE

Public reporting burden for this collection of information is estimated to average 1 hour per response, including the time for reviewing instructions, searching existing data sources, gathering and maintaining the data needed, and completing and reviewing the collection of information. Send comments regarding this burden estimate or any other aspect of this collection of information, including suggestions for reducing this burden, to Washington Headquarters Services, Directorate for Information Operations and Reports, 1215 Jefferson Davis Highway, Suite 1204, Arlington, VA 22202-4302, and to the Office of Management and Budget, Paperwork Reduction Project (0704-0188), Washington, DC 20503.

1. AGENCY USE ONLY *(Leave blank)*	2. REPORT DATE	3. REPORT TYPE AND DATES COVERED
	December 1990	Master's Thesis

4. TITLE AND SUBTITLE

DEBRIS PRODUCTION IN HYPERVELOCITY IMPACT
ASAT ENGAGEMENTS

5. FUNDING NUMBERS

6. AUTHOR(S)

Stephen Karl Remillard, Captain, USAF

7. PERFORMING ORGANIZATION NAME(S) AND ADDRESS(ES)

Air Force Institute of Technology, WPAFB OH 45433-6583

8. PERFORMING ORGANIZATION REPORT NUMBER

AFIT/GSO/ENS/90D-15

9. SPONSORING/MONITORING AGENCY NAME(S) AND ADDRESS(ES)

10. SPONSORING/MONITORING AGENCY REPORT NUMBER

11. SUPPLEMENTARY NOTES

12a. DISTRIBUTION/AVAILABILITY STATEMENT

Approved for public release; distribution unlimited

12b. DISTRIBUTION CODE

13. ABSTRACT *(Maximum 200 words)*

This study reviews laboratory experiments on hypervelocity impacts and applies the results from those experiments to predict the mass of debris produced, the number of particles, and the size distribution of the debris particles produced in an ASAT engagement using kinetic energy weapons. The three possible types of hypervelocity collisions are discussed and parameters are provided that will help predict what type of collision will occur between a given projectile and a target satellite. Once the collision type is determined, various equations are supplied which can be used to calculate debris mass, etc. Next, a notional attack between a miniature homing vehicle, similar to the one used in the successful F-15 launched ASAT, and two different satellites are examined to show the methodology for predicting the results of an ASAT engagement. Finally, suggestions are presented which can help a commander minimize the creation of debris, and thus minimize the long-term collision hazard for spacecraft resulting from ASAT engagements using kinetic energy weapons.

14. SUBJECT TERMS

ASAT Engagements, Hypervelocity Impacts,
Satellites, Debris Production, Rorsat, Solwind

15. NUMBER OF PAGES

98

16. PRICE CODE

17. SECURITY CLASSIFICATION OF REPORT	18. SECURITY CLASSIFICATION OF THIS PAGE	19. SECURITY CLASSIFICATION OF ABSTRACT	20. LIMITATION OF ABSTRACT
UNCLASSIFIED	UNCLASSIFIED	UNCLASSIFIED	UL